Computers & Industrial Engineering 162 (2021) 107727

Contents lists available at ScienceDirect

Computers & Industrial Engineering

journal homepage: www.elsevier.com/locate/caie

A framework for the resilience analysis of complex natural gas pipeline networks from a cyber-physical system perspective

Antonio Marino [a], Enrico Zio [a,b]

[a] Politecnico di Milano – Dipartimento di energia, Italy
[b] Mines Paristech, France

ARTICLE INFO

Keywords:
Resilience analysis
SCADA networks
Gas pipeline transmission networks
Complex Networks
Maximum Flow Algorithm
Thermal-Hydraulic simulation

ABSTRACT

The vulnerability of gas pipeline networks to physical and cyber-attacks calls for a resilience analysis based on models, capable of quantifying the network robustness and recovery from failures.

This work proposes an original resilience analysis framework for a complex gas pipeline transmission network, considering the cybernetic interdependence of the physical gas pipeline network with the SCADA system. The maximum flow algorithm computes the gas network supply capacity and when a failure occurs, the pressure of the network nodes and the gas supply capacity change, leading to dissatisfaction of customer demands. The framework allows quantifing the value of resilience through specific performance metrics.

The SCADA communication network, implemented in Network Simulator®, provides the necessary information regarding the delay of data packets coming from the sensors located along the pipelines. The packet delay value allows to evaluate the actual time at which the SCADA system blocks the remote control valves, ready to keep the pipelines under pressure when a failure occurs.

Important insights on the resilience model are obtained through a systematic sensitivity analysis (SA) framework, customized for gas pipeline transmission networks. Specifically, we investigate the influence of model inputs to the network robustness and recovery uncertainty. The effects of individual parameters and groups formed by inputs with similar functionalities provide useful information, such as to what extent the supervisory SCADA system interconnection affects the degradation and the recovery process of the physical gas pipeline network.

The results of the case study confirm, as expected, that gas transmission networks are vulnerable to both cyber and physical failures, pointing at the need for systemic methods of analysis for managing the system resilience.

1. Introduction

The natural gas pipeline transmission network is a Critical Infrastructure (CI) (Zio & Sansavini, 2013). The interruption or shortage of natural gas supply could bring significant damage to economy and societal stability of a Country (Ebrahimy, 2014). In operation, the Supervisory Control and Data Acquisition (SCADA) system monitors and controls the conditions of the system, such as temperature, flow rate and pressure inside the pipelines. A SCADA system is made of computers, controllers, instruments, actuators, networks and interfaces that manage the control of automated industrial processes and allow analysis through data collection by monitoring sensors (Kim, 2010; Hildick-Smith, 2005).

The interconnection between gas pipeline networks and SCADA communication networks ensures continuity of service, safety monitoring and prevention of economic loss. If on one hand, the interconnection brings significant benefits, on the other hand, they can channel-in vulnerabilities in the system. The dependency of the natural gas service on Internet information technology has caused vulnerabilities to cybernetic attacks.

One of the most famous cybernetic attacks date back to the year 2000 in Maarochy Shire, where 800,000 L of raw sewage have been released into local parks and rivers, causing death of marine life and discoloration of water. More recently, in 2016, cyber attacking of the Smart Grid Units (SGU) has caused the Ukraine's blackout where for three hours, 80,000 customers did not benefit electricity (Abrams & Weiss, 2008; Sayfayn; Queiroz et al., 2011).

The main concern for critical infrastructures is, then, their resilience. Resilience is defined as the ability to resist or absorb damages in a way to maintain acceptable levels of system performance and to quickly recover the nominal functionality (Attoh-Okine, 2016; Filippini & Silva, 2014; Wadhawan & Neumann, 2018).

E-mail addresses: antonio2.marino@mail.polimi.it (A. Marino), enrico.zio@polimi.it (E. Zio).

https://doi.org/10.1016/j.cie.2021.107727
Received 7 February 2021; Received in revised form 30 July 2021; Accepted 3 October 2021
Available online 6 October 2021

Nomenclature

AODV	Ad-hoc On-demand Distance Vector
A_{or}	Cross sectional area of the orifice (m^2)
b_{ij}	Recovery speed parameter of the pipeline (i,j)
C_D	Dimensionless discharge coefficient
CBR	Constant Bit Rate
CDF	Cumulative distribution function
CI	Critical Infrastructure
d	Base knowledge about a model input parameter
d'	Alternative knowledge about a model input parameter
D_{ij}	Diameter of the pipeline (i,j) (m)
DDOS	Distributed Denial Of Service
E	Expected value symbol
g_{deg}	Network degradation function
g_{rec}	Network recovery function
$G_{RecCap}(T_{rec})$	Capacity recovery function output computed at T_{rec} (m^3)
$G_{RobCap}(\overline{T}_{det})$	Capacity robustness function output computed at $\overline{T}_{det}$ (m^3)
K	Promptness parameter of the SCADA system to detect failures
L_{ij}	Length of the pipeline (i,j) (m)
MCM/d	Million cubic meter per day
M(E_v)	Magnitude of the event E_v
m	Pressure degradation rate parameter (psi/s)
$\dot{m}_{hole}$	Mass flow rate (kg/s)
$mf_{t=0}$	Initial maximum flow of the gas transmission network (MCM/d)
mpd	Maximum packets delay parameter (s)
MAOP	Maximum allowable opearting pressure (psi)
NS	Network Simulator
N_s	Number of samples of each input parameter
P_{detect}	Degradation pressure detected by the SCADA system (psi)
$P_{fin.real}$	Effective pressure retained in the pipeline before recovery (psi)
$P_{initial}$	Node pressure before failure in a steady-state condition (psi)
$P_{(initial(i,j))}$	Pressure of the pipeline (i,j) before degradation event (psi)
PDF	Probability density function
Pr(E_v)	Probability of occurence of the event E_v
PSA	Probabilistic Safety Assessment
Q_{ij} (t)	Pipeline (i,j) transmission capacity (Nm^3/h) at a generic time t
$Q_{ij,0}$	Pipeline (i,j) initial transmission capacity at time t = 0 (Nm^3/h)
RCV	Remote Control Valve
RPI	Resilience Performance Index
RTU	Remote Terminal Unit
SA	Sensitivity Analysis
SCADA	Supervisory Control and Data Acquisition
T_{cont}	Temperature inside the pipeline (K)
τ	Time constant (s)
t	Time (s)
t_{dest}	Time that gas takes to reach the delivery node (s)
$t_{effective}$	Effective SCADA failure detection time (s)
t_r	Time step (s)
$\overline{T}_{det}$	Mean detection time of the failure (s)
T_{det} (i,j)	Detection time for the pipeline (i,j) (s)
T_{rec}	Recovery observation Time (s)
TCP	Transmission Control Protocol
UDP	User Datagram Protocol
Var	Variance symbol
V_{gas}	Natural gas recovery speed (m/s)
X_i	*ith* model input parameter
q_α	Quantile q of order α
x_i^j	*jth* sample of the *ith* input parameter
Y	Generic model output
Z	Gas compressibility factor

Greek letter parameters

δ	Conversion coefficient for pipeline capacity calculation
γ	Isontropic coefficient
λ	Pipeline pressure increase logarithmic rate (psi/s)
μ	Mean value of a generic probability distribution
$\eta^2_{gr_j}$	Closed-order sensitivity index of the *jth* group of parameters
η^2_i	First-order sensitivity index of the *ith* input parameter
η^2_{Ti}	Total-order sensitivity index of the *ith* input parameter
$\varphi(t)$	System performance function at time t
Ψ	Dimensionless factor for gas velocity
σ	Standard deviation of a generic probability distribution
θ	Pipeline pressure increase linear rate (psi/s)

Several works have considered the analysis of resilience systems with interdependence between physical and communication networks. The works of the authors in (Korkali, Veneman, Tivnan, Bagrow, & Hines, 2017) and (Chopade & Bikdash, 2012), for example, model interdependence of an electric power network and a communication network. Specifically, authors in reference (Korkali et al., 2017) analyze three cascading failures models to evaluate the interdependent network resilience: Erdos-Renyi (ER) model, Small World (SW) model and Scale-free (SF) model.

The authors in (Chai et al., 2016; Gao et al., 2015; Hu et al., 2011; Michael et al., 2016), use percolation theory to analyze the robustness of CIs and evaluate the importance of the different network nodes by means different centrality measures. The author in (Carvalho et al., 2009), using the percolation theory (Linkov et al., 2019; Goel et al., 2011; Huang et al., 2015), performs the robustness analysis of the trans-European gas pipeline network from a topological point of view. The author proposes an analysis model based on the maximum flow method to estimate the tolerance of the network to failures. In these works, the approach by graph theory leads to neglecting the physical details of how the pressure and the gas flow change in the network pipelines.

Also, inevitably, models based on graph theory cannot fully consider important functional parameters of the information transmission process like the bit rate, the type of transport layer protocol (UDP or TCP), the radio frequency of the sensors and the type of routing algorithm, such as the AODV protocol. Many efforts have been done to overcome this problem. Reference (Wadhawan & Neuman, 2016) attempts to present a more realistic model of the interdependence between the gas pipeline network and the SCADA system, using Network Simulator® to represent a more realistic communication network. The authors propose the Time to Criticality (TTC) to quantify the time for an event to reach the failure state, considering the process response of the SCADA system; a resilience analysis method for a gas pipeline network is provided but considering only cyber attacks while ignoring physical failures.

Another approach taken for modeling the complexity of interdependent networks, is based on agent-based models. Reference (Gonzalez De Durana, Barambones, Kremers, & Varga, 2014) proposes an agent-based model to capture the complexity of interaction of the power grid with other energy networks. Similarly, reference (Kremers,

Gonzalez De Durana, & Barambones, 2013) proposes an agent-based model of a smart microgrid. Inevitably, in this approach the results are dependent on the assumptions on the behavior of the agents, whose modeling difficulty increases with the complexity of the systems and their interactions.

In this work is developed an innovative resilience model that considers the complexity of gas networks, capable to predict system response (Iooss & Saltelli, 2015) and to quantify the value of resilience using performance metrics (Ganguly, Bhatia, & Flynn, 2018). The method integrates thermal–hydraulic simulation, graph theory and wireless network simulation. Specific functions are introduced to model the pipelines degradation and recovery.

The analysis method proposed in this work aims to link mathematical theoretical models and the complex physical reality of critical infrastructures. The method consists of four modules: the complex network modeling module, the physical failure scenarios modeling module, the cybernetic failure scenarios modeling module and the complex network resilience analysis module.

The goals of these modules are:

(1) *complex network modeling*: to build the physical gas pipeline transmission network and to simulate the response of the SCADA system under normal conditions and under DDoS attack;
(2) *physical failure scenarios modeling*: to model the network evolution if physical failure scenarios occur in the network and to evaluate the magnitude of the consequences to proceed with a resilience analysis.
(3) *cybernetic failure scenarios modeling*: to model the complexity of a pressure integrity cyber attack, evaluating the magnitude of the most threatening consequences.
(4) *network resilience analysis*: to assess the resilience of the network for the most severe failures.

Sensitivity analysis can be exploited to extract information from resilience models allowing to obtain useful information on the bottlenecks of the systems and understanding which parameters have a dominant effect on the system response. Such information can guide decision making for planning and system operation (Lv et al., 2019; di Maio et al., 2014; Makowski, 2013; Pianosi et al., 2015; Saltelli et al., 2004). One of the main goals of SA is to determine the key uncertainty drivers of the model output uncertainty (Saltelli, 2007). Various sensitivity measures have been developed. One of the most commonly used global sensitivity analysis methods is the variance-based sensitivity approach of Sobol (Sobol, 1993), which has achieved great success in various applications, such as nuclear safety assessments (di Maio et al., 2014, 2017; Zio and Pedroni, 2010; Zio and Pedroni, 2012) and ecological models (Perz et al., 2013; Cariboni et al., 2007).

Applying sensitivity analysis methods to resilience models for gas pipeline transmission networks can be challenging because they are inherently dynamic, time-dependent models that involve various parameters characterizing both the physical pipeline network and the complex SCADA cyber-system that governs its functioning. Although some SA works have been developed for gas transmission networks (Zeng et al., 2018; Homma and Saltelli, 1996), to the best of our knowledge, sensitivity analysis on resilience models for complex networks has not yet been considered.

In this work is developed a comprehensive sensitivity analysis for the resilience model of gas pipeline transmission networks. Guidelines are provided to categorize groups of parameters and to study dynamic models using the variance-based SA method.

The framework for the sensitivity analysis is divided into four stages: analysis of the model outputs, parameter prioritization, trend identification and "what-if" analysis of the modified value of information in terms of mean and quantiles. The goals of these stages are:

(1) *analysis of the model outputs*: to give insights about the network resilience by looking at the output distribution;
(2) *parameter prioritization*: to identify single parameters and groups of parameters that, given the input uncertainty distributions and ranges, would lead to the greatest reduction in the variability of the model output (Saltelli & Tarantola, 2002);
(3) *trend identification*: to provide model insights to understand if the increase or decrease of an input parameter has positive or negative effects on the outputs (Borgonovo, Lu, Plischke, Rakovec, & Hill, 2017);
(4) *"what-if" analysis*: to give indications on what happens to the outputs of the resilience model when acquiring more knowledge on the inputs (Schreider et al., 2015; Koch et al., 2009; Peterson et al., 2009).

The overall methodology framework for natural gas pipeline transmission networks is shown in Fig. 1.

To summarize, the research objectives of this work are:

- Develop a resilience analysis framework to quantify the robustness and the recovery of a complex gas pipeline transmission network, considering the interdependence with a SCADA system.
- Develop a sensitivity analysis framework to get important insights on the network resilience model for supporting the decision making.
- Assess whether the proposed frameworks are flexible and adaptable to gas transmission networks composed by many nodes and pipelines.
- Overcome the complexity of the time-dependency of the gas network recovery to estimate the Sobol sensitivity indices of the first-order and the total-order for the parameters of the gas pipeline network recovery model.

2. Complex network modeling

2.1. SCADA communication network model

The communication network model is developed to simulate the SCADA system functioning. Pipelines are divided in segments and each of them can be isolated due to maintenance or failures, by shutting down block valve stations situated every 20/30 km from each other. In each segment of pipeline there are many sensors that transmit by RTUs the pipeline gas information, such as pressure, flow and temperature, from the pipeline to the master control center (NetSCADA, 2010).

For the development of the communication network, we used the WLAN technology to link the SCADA monitoring center to the RTUs located on the segment of the pipeline. For a clear illustration, Fig. 2 shows a segment of pipeline that transmits information to a host computer situated at the SCADA control center via communication pathways. The letters "*f,p,t*" represent the functions of the RTU of monitoring flow, pressure and temperature, respectively; "*a*" is the alarm function of the RTU.

To develop the SCADA network, a wireless mesh network approach is adopted (Mohamed et al., 2008; Fall and Varadhan, 2011) using Network Simulator® (NS2). NS2 is an open-source event-driven simulator designed specifically for communication networks. It is one of the most widely used open-source network simulators (Issariyakul & Hossain, 2012). It contains modules for numerous network components such as routing, transport layer protocol and application protocol. To investigate network performance, researchers can simply use an easy-to-use scripting language to configure a network and observe results generated by NS2.

The input parameters to be included in the model are:

a. Number of RTUs to be considered
b. Number of communication nodes used as pathway nodes
c. Data rate

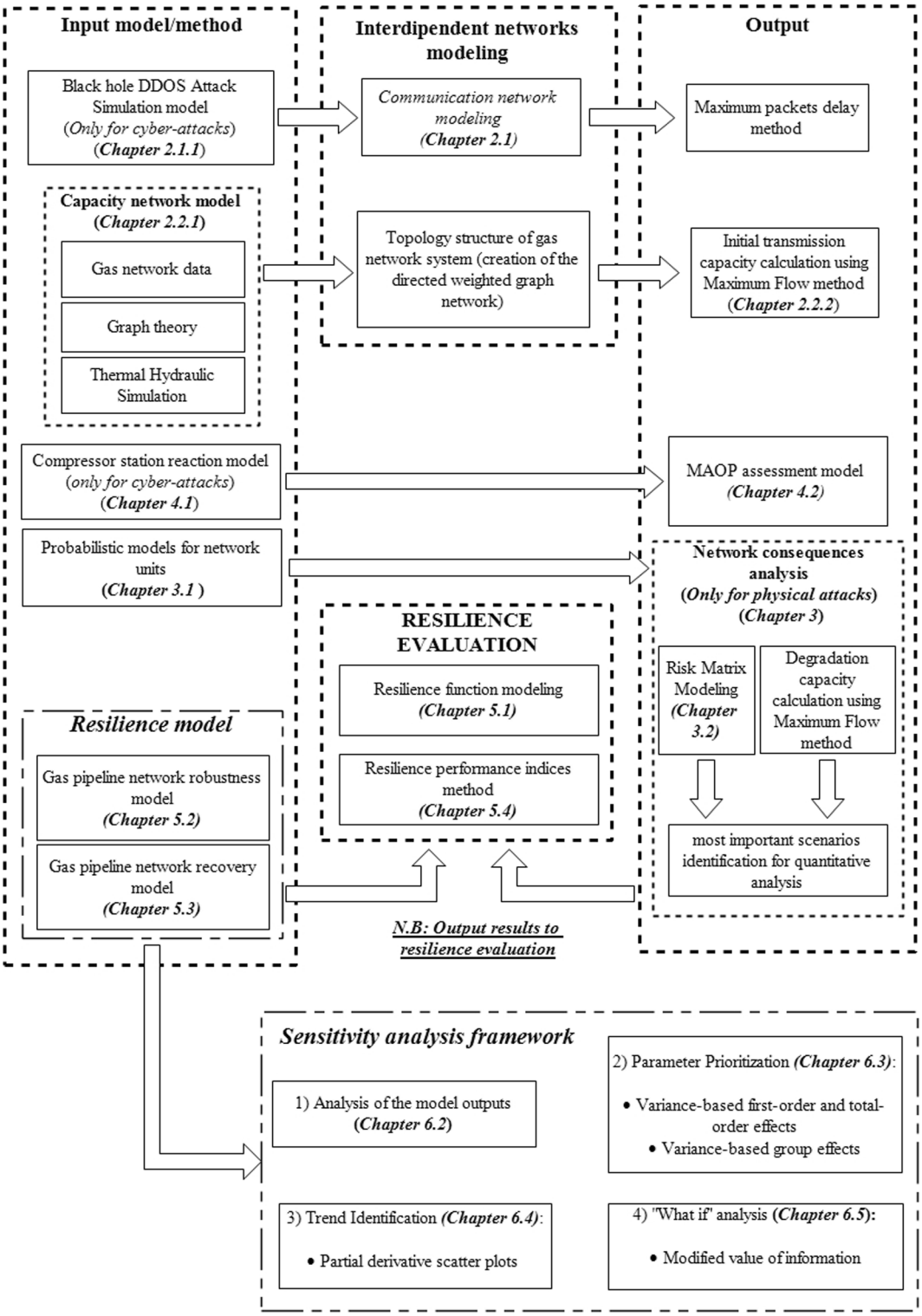

Fig. 1. Methodology framework for gas transmission networks integrated assessment.

d. Radio frequency for each RTU
e. Type of transport layer protocol
f. Type of traffic generation
g. Distance of the communication nodes by each other
h. Routing Protocol
i. Time horizon for the simulation

The input parameters are obtained from the analysis of real SCADA networks and used in the proposed model. The simulation results are obtained using an application, called *NSwireless*®.

This software package considers wireless networks developed in Network Simulator® and allows getting important information on the packets sent by the RTUs to the control center, such as the average packets delay, the maximum packets delay and the percentage of dropped packets during the simulation. If a failure occurs on the network, an alarm signal is transmitted by the RTUs for avoiding the

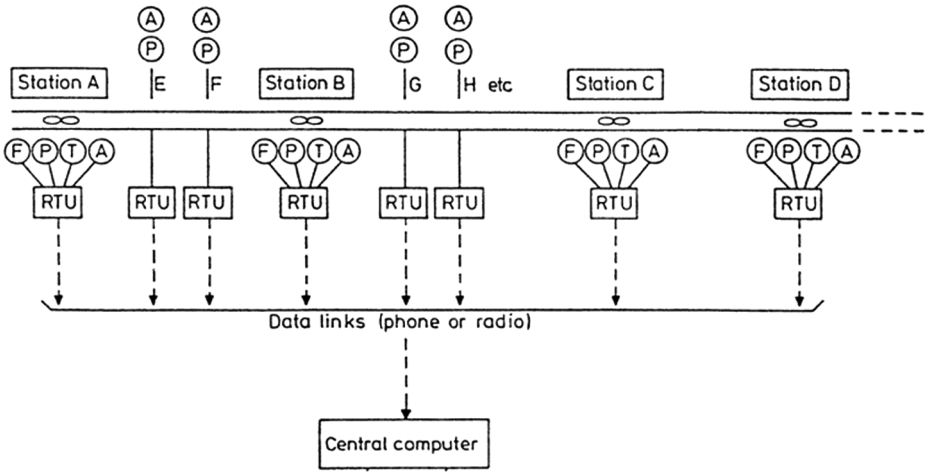

Fig. 2. Schematic overview of pipeline computer-based monitoring system (McAllister, 2005).

depressurization of the pipelines involved.

Through remote control, the SCADA control center must intervene on the block valves for keeping pipelines under pressure. Considering the delay of the data packets allows to evaluate the real intervention time of the SCADA system on the block valves, calculating the final pressure retained inside the pipeline. In our analysis the type of dealy assumed is the maximum packets delay, for conservative reasons.

The *alarm information* in this work is the indication that the pressure has dropped by −10% compared to the initial pipeline set point pressure. The final pressure inside the pipeline, then, depends also on the efficiency of failure detection of the SCADA communication network: the greater the delay of the information, the lower the pressure inside the pipeline will be, when the system acts on block valves.

2.1.1. Modeling DDoS black hole cyber-attack

Black hole attack is a type of DDoS attack that concerns the wireless sensor networks (Pelechrinis, Iliofotou, & Krishnamurthy, 2011). Some of the malicious nodes enter in some transmission paths and start dropping the legitimate packets. In this way, such nodes play the role of black holes. In this work the modeling of a black hole DDoS computer attack is composed of two parts:

(1) modeling the compromise of a percentage of the communication nodes
(2) extract the information concerning the maximum packets delay.

2.1.2. Pressure integrity and DDOS black hole cyber-attack scenario description

The pressure integrity attack scenario (Wadhawan and Neumann, 2018; Gonzalez De Durana et al., 2014) is a type of cyber-attack that aims to damage the pipelines due to overpressure. The description of the attack is as follows:

(1) First, the attacker compromises the RTUs and blocks the RCVs present along the pipeline, preventing the correct information from reaching the SCADA control center. While the pipeline pressure increases, the attacker sends a misleading message with wrong pressure information to the SCADA system. Operators at the control center will not be able to know the real pressure inside the pipeline under attack.
(2) After a certain time that the attacker has blocked the RCVs, the delivery pressure at the destination node changes. The pressure inside the pipeline increases due to the RCVs closure and the delivery pressure of the downstream node decreases. SCADA system believes that the pressure decreasing of the delivery node is due to an increase of the gas demand in the network. The consequence could be catastrophic, because at this point the SCADA sends a message to the compressor station to increase the delivery pressure for guaranteeing the supply of gas in the network. If MAOP is reached, the pipeline breaks due to overpressure.
(3) After a certain time, the SCADA detects that something is wrong because the pressure at the delivery node does not grow. The SCADA system sends signals to RTUs and compressor station to increase the information about the pipeline segment. However, the information flow is not efficient because the attacker has performed a DDoS black hole attack.

Operators at the SCADA control center must call the operator at the compressor station to take safety procedure (Gas Pressure Regulation and Overpressure Protection).

2.2. Physical network model

2.2.1. Network capacity model

A network capacity model has been developed in a similar way of (Su et al., 2018) to describe its structure and transportation capacity. The model is a directed weighted graph, in which pipelines are represented as arcs of given capacity weights and connect nodes representing compressor stations, LNG terminals, natural gas storages and demand nodes.

The directions of gas flow and the values of the pressure at the nodes are obtained using the Pipe Flow Expert® software, based on a steady-state thermal–hydraulic simulation.

The input values (Su et al., 2018) to insert in Pipe Flow Expert® are:

(1) Data of customers demands
(2) Gas pressure at the source points
(3) Pipeline diameters

The capacity weigths of the arcs are calculated in accordance to the GTE report in (Linkov et al., 2019; Transmission Europe), based on the relationship between the pipeline capacity Q and the pipeline diameter D:

$$QD^{-\delta} \tag{1}$$

where D is the diameter of the pipeline, in meters; Q is the estimated capacity of the pipeline, in MCM/h; δ is a constant conversion coefficient equal to 2.59.

2.3. Transmission capacity calculation

The capacity of the gas pipeline transmission network is computed through the maximum flow method by the Ford-Fulkerson algorithm (Lloyd, Bondy, & Murty, 2007). In this work, the maximum flow is a metric to measure the supply capacity and the system performance of the network due to its extensive application in practice and its simplicity to adapt to other problems.

Consider a directed network G (V, E), where V denotes the set of vertices and E represents the set of arcs in G. Each link $(i,j) \in E$ is associated with a nonnegative flow variablef_{ij}. The capacity of each link (i,j) is denoted by u_{ij}.

Let o and d (o, $d \in$ V) be the origin node and the destination node of network G, respectively. The maximum flow problem is to send as much flow as possible from o to d, while the flow f_{ij}along the link (i,j) cannot exceed its capacity u_{ij}.

Mathematically, the problem can be formulated in the following form:

$$\begin{aligned} &\max && f_{od} \\ &s.t. && \sum_{(i,j)\in E} f_{ij} - \sum_{(i,j)\in E} f_{ji} = 0 \qquad for\ \ each\ \ j \in V\backslash\{o,d\} \\ &0 \le f_{ij} \le u_{ij}, && \forall (i,j) \in E. \end{aligned}$$

Generally, in gas networks there are multiple sources and sinks. The maximum flow method can be extended by considering a “supersource” and a “supersink” node, which are connected respectively to all the sources and sinks by edges of infinite capacity; introducing a supersource o (virtual source node) with edges (of unlimited capacity) directed to all source nodes o_1,o_2,…, $o_k$and a supersink d (virtual sink node) with edges (of unlimited capacity) connected to it from all sink nodes d_1,d_2,…, d_k. The problem of maximising the total value of the flow from all sources is the same as that of maximising the value of the flow from o to d (Praks, Kopustinskas, & Masera, 2015).

3. Modeling of physical failure scenarios

The capacities of the pipelines involved in a failure could decrease during degradation. When a failure occurs, the transmission capacity of the network is reduced if it is not robust to that failure. The maximum flow algorithm allows to compute the transmission capacity of the network also during degradation conditions. To quantify the consequences, it is first necessary to model the failure of the nodes and pipelines. The probabilistic network component failures model is developed based on references (Gas Pressure Regulation and Overpressure Protection).

3.1. Probabilistic models for network units

3.1.1. Probabilistic model of pipelines failure

Pipelines may fail due to spilling (small or large leakage) and interruption (rupture or wrong operations). A pipeline failure consequence is here modelled as the reduction of the pipeline capacity to zero (SCADA detects failure and blocks the pipeline) (Praks et al., 2015). According to the EGIG report (EGIG, 2011, 2011), the average failure frequency of a European gas transmission pipeline is 3.5×10^5/(km·year).

3.1.2. Probabilistic model of compressor stations failure

The failure of the compressor station refers to the failure of the compressors inside it. When degeneration leads to a failure of a compressor, the compressor station continues working but the surrounding pipelines capacity is reduced. More precisely, a compressor station failure reduces the inlet pipeline and the outlet pipeline capacity by 20%. This estimate is based on known operational cases (Praks et al., 2015). It is assumed that the annual failure probability of a compressor station is 0.25.

3.1.3. Probabilistic model of natural gas storages failure

Capacity reduction and supply interruption of gas storages are mainly caused by facility failure and continuous withdrawal. In case of a gas storage failure, it is assumed that the capacity of the pipeline connected to the gas storage is reduced to zero (Kopustinskas & Praks, 2014). According to expert knowledge (Ouyang, 2014), we set the annual failure probability of the gas storage to 0.10.

3.1.4. Probabilistic model for LNG terminals

Capacity of a LNG terminal is mantained within a normal range but in a few situations significant reduction of supply capacity, even interruption, may happen. In case of a LNG component failure, it is assumed that the capacity of the pipeline connected to the LNG terminal is reduced to zero. According to literature indications (Jung, Cho, & Ryu, 2003), we set the annual failure probability of the LNG terminal to 0.15.

3.2. Risk matrix modeling

Risk matrix model is a well defined model in risk assessment (Ganguly et al., 2018; Wilkinson and David, 2009). It is used to define the level of risk R considering the probability $Pr(E_v)$ of occurrence of hazardous events E_v and the magnitude $M(E_v)$ of the consequences.

Fig. 3 shows a risk matrix 5×5, where each cell contains a risk value calculated as the product $M(E_v) \times Pr(E_v)$. The values of the probability of $Pr(E_v)$ and $M(E_v)$ are partitioned into five categories, based on probability ranges and loss of network capacity, respectively.

In this work, to assess the failure scenarios to be considered for the resilience analysis, the probability examined in the risk matrix is the probability of failure of the network units; the value of magnitude, instead, is the value of the transmission capacity of the network when the network is in a state of degradation due to the unit failure under analysis.**

4. Modeling cybernetic failure scenarios

Pressure integrity cyber-attack is one of the most feared cyber-attacks in the Oil & Gas field. Attackers affect the gas delivery by maliciously increasing the gas pressure through a pipeline (Zhang, Mahadevan, Sankararaman, & Goebel, 2018). If the pressure reaches the maximum allowable overpressure (MAOP), significant economic losses due to the non-provision of the service or, in the worst case, environmental disasters can take place.

4.1. Pressure reaction model of the compressor station

We considered different models of pressure increasing inside a pipeline linked to a compressor station where the latter has been instructed to increase the gas delivery pressure (Zhang et al., 2018).

Different types of curve are reported in Fig. 4 assuming linear and logarithmic responses. We suppose that the compressor station can increase the pressure inside an adjacent pipeline linearly or logarithmically with different types of rate (θ and λ for linear and logarithmic assumption, respectively).

4.2. Evaluation of reaching the MAOP

Until the natural gas reaches the delivery node with high pressure, the SCADA system is unable to find the network irregular functioning. As said in Section 2.1.2, after a certain time, network operators expect that the pressure at the delivery node increases but this does not happen due to the malicious closure of RCVs. After this period, the compression station decides to implement safety procedures.

Given the pipeline length between the compressor station and the delivery node, Pipe Flow Expert® computes the gas velocity inside the pipeline. The delivery time is calculated as the pipeline length divided by the gas velocity. If the pressure reaches the MAOP, the pipeline, then,

Risk Matrix					
Probability \ Magnitude	1 Very Low (0- 5%)	2 Low (5- 10%)	3 Medium (10- 25%)	4 High (25- 50%)	5 Very High (>50%)
5 Very Probable (0.75<P<=1)	5	10	15	20	25
4 Probable (0.5<P<=0.75)	4	8	12	16	20
3 Possible (0.10<P<=0.5)	3	6	9	12	15
2 Unlikely (0.05<P<=0.10)	2	4	6	8	10
1 Rare (P<=0.05)	1	2	3	4	5

Fig. 3. Risk matrix model.

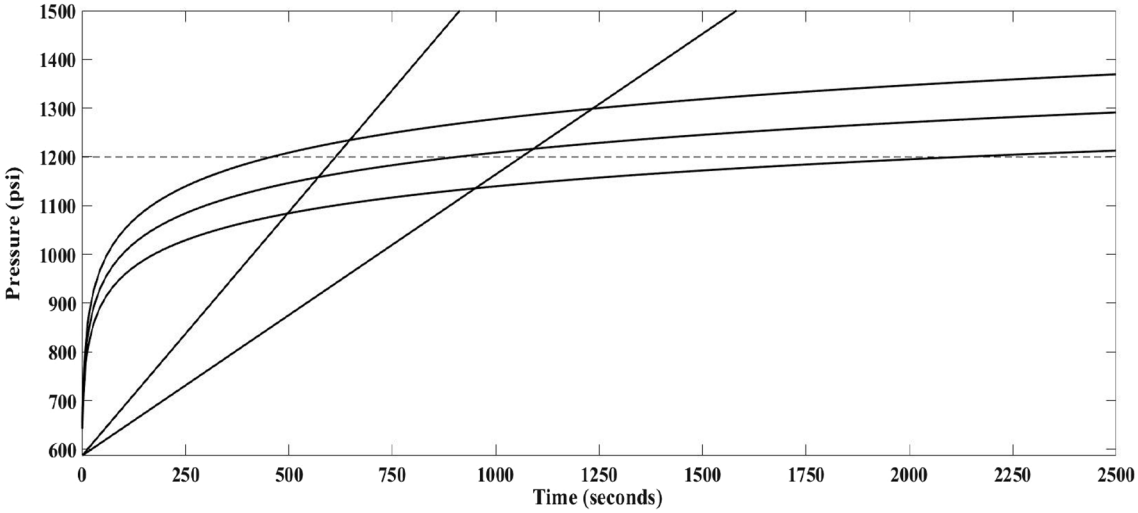

Fig. 4. Different types of pressure increasing functions inside the outgoing pipeline adjacent to the compressor station (dash line is the MAOP).

fails.

It is important to highlight that the loss of service, and therefore the economic loss due to the reduction in supply, does not constitute the most significant damage. The loss of service may lead to serious economic damages but the reaching of the MAOP can lead to loss of human life as well as an environmental disaster.

Among the events that may occur, the most significant are:

(a) Spilling
(b) Jet Fire
(c) VCE (Vapour Cloud Explosion)

For provideing some information to increase the cyber-robustness of the networks from cybernetic failures, it is necessary to analyze what could be the consequences of these accident events.

4.2.1. Spilling

The mass flow rate of gas through an orifice can be calculated using the following expression, obtained from the mechanical energy balance by assuming isoentropic expansion and introducing a discharge coefficient (Casal, 2008c):

$$\dot{m}_{hole} = A_{or}\ C_D P_{cont}\ \psi \left(\gamma \left(\frac{2}{\gamma+1} \right)^{\left(\frac{\gamma+1}{\gamma-1}\right)} \frac{C_D}{Z\ T_{cont}\ R\ 10^3} \right)^{1/2} \tag{2}$$

where

- m_{hole} is the mass flow rate (kg s^{-1})
- γ is the isentropic coefficient (1.4 for natural gas)
- $C_{(D)}$ is a dimensionless discharge coefficient
- $A_{(or)}$ is the cross-sectional area of the orifice (m^2)
- Z is the gas compressibility factor at the inlet pressure P_{cont} (Pa) and temperature T_{cont} (K) of the pipeline. For ideal gas, Z = 1
- Ψ is a dimensionless factor that depends on the velocity of the gas. For sonic gas velocity, $\Psi = 1$

A pipeline rupture is assumed, according with (Grossel, 2001), as

20% and 100% of the pipeline diameter. In a conservative way, natural gas is assumed as an ideal gas (Z = 1) and flow is sonic (Ψ = 1).

4.2.2. Jet fire

The immediate ignition of a pipeline release may generate a jet fire, which produces significant heat irradiation effects.

Danegerous irradiation values due to fire exposure are:

(1) 2.5 kW/m^2 for the equipment
(2) 12.5 kW/m^2 for the people.

It is necessary to calculate the distance of exposure to these values of irradiation, to evaluate the danger of the jet fire accident event. The spilling diameter is assumed about 20% of the pipeline diameter. In the reference work (Casal, 2008a), the reader can find the appropriate formulas to model a jet fire.

4.2.3. Vapor Cloud Explosion (VCE)

Explosions are associated with a very fast release of energy. In case of VCE a vapor cloud is formed due to the loss of containment of a certain mass of a flammable gas.

For an explosion to occur, there must be a delay in ignition; if there is a significant delay, it is possible that a sufficiently large cloud of a fuel – air mixture will develop. In this work, for conservative assumptions, the time spent to form a mixture of natural gas with the surrounding air has been taken equal to the time of detection of the exceedance of the MAOP in the pipeline.

If an explosion occurs, the mechanical energy of the explosion constitutes a blast wave that moves at a certain velocity through the athmosphere. This phenomenon causes an overpressure. To obtain the values of overpressures at a distance of 100 m from the origin of the explosion, the Viekema Method is adopted (Casal, 2008b).

5. Resilience modeling

5.1. Resilience function

To quantify the system resilience R, we introduce a system resilience function $\varphi(t)$to describe the system behavior at time t (Henry & Ramirez-Marquez, 2012). In this work, we adopt a resilience function $\varphi(t)$ based on the maximum gas supply capacity to measure the system performance. The distinct stages to characterize the transition of the system over time are shown in Fig. 5.

The area underlying the function identifies the network capacity to absorb and recover failures.

5.2. Gas pipeline network robustness model

The robustness of a gas pipeline transmission network is here interpreted as the ability to maintain its basic functionality even under failures of some components and systems (Su et al., 2018). The network robustness capacity is the amount of natural gas that the network is still capable of processing under the failure scenario.

Some accident scenarios involve multiple pipelines, which are blocked by RCVs to avoid their depressurization (Johansson, Östling, & Jagschies, 2018). Each pipeline involved in the failure event is blocked when a certain threshold level of depressurization is reached. The time at which the depressurization level inside the pipeline is detected by the SCADA network is called *failure detection time*. For simplicity, the multiple failure detection time is assumed as the average of the failure detection times of the involved pipelines. The lack of information about the rate of depressurization inside pipelines leads us to consider a linear depressurization, for simplicity.

Let $\mathscr{S}$ denote the set of the pipelines and (i,j) the generic pipeline link where i and $j \in \mathscr{S}$. The failure detection time for a generic pipeline whose initial and final nodes are i and j, respectively, is computed as follows:

$$T_{det}(i,j) = \frac{K \cdot P_{initial(i,j)}}{m} + mpd \tag{3}$$

where

- $P_{(initial(i,j))}$is the initial pipeline pressure (psi) for pipeline link (i,j);
- m is the linear (constant) pressure degradation rate inside the pipeline (psi/s);
- K is the promptness parameter of the SCADA system; when the initial pressure drops by$(-K \cdot P_{(initial)})$, an alarm is sent by the communication network, and the pipeline is blocked and kept under pressure. In this work, we want to remind the reader, a K value of 0.1 is assumed;
- mpd is the maximum packets delay (s); when the pressure inside the pipeline drops by$(-K \cdot P_{(initial)})$, it is assumed that the alarm message has a delay equal to mpd before the SCADA system acts on the blocking valves.

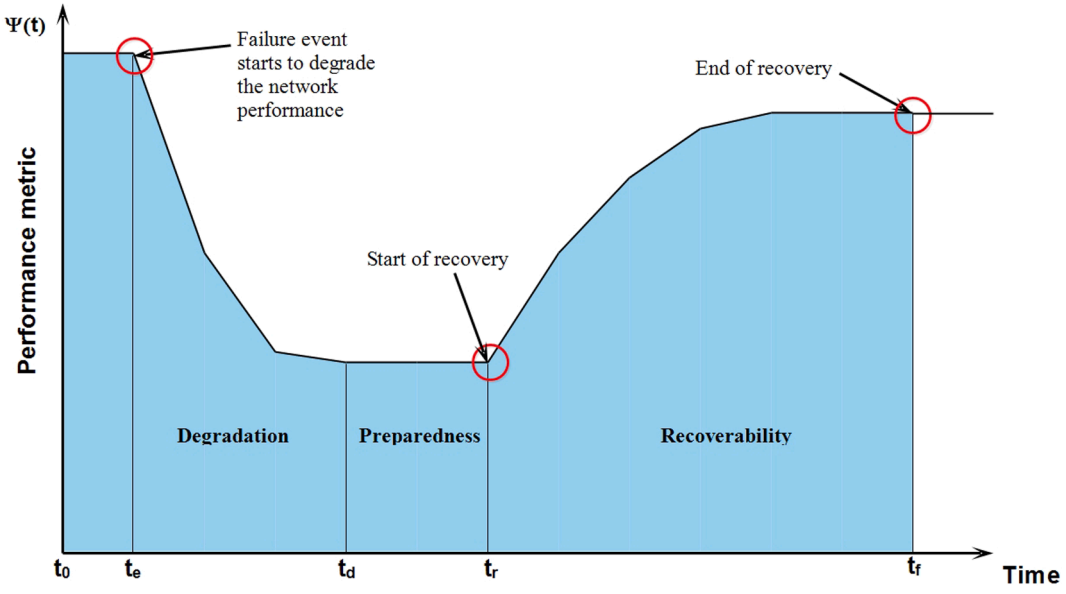

Fig. 5. System resilience function over time (Zhang et al., 2018; Henry and Emmanuel Ramirez-Marquez, 2012).

Obviously, we must consider the pressure drop inside the pipeline. Therefore, the value of the pipeline *(i,j)* pressure is assumed to have the value of the end node *j* to simplify the problem. The pressure drops of the pipeline are automatically taken into consideration by Pipe Flow Expert®. This assumption avoids the development of too complex equations.

Considering a constant depressurization, the degradation function $g_{deg}(t)$ is defined as follows:

$$g_{deg}(t) = mf_{t=0} \cdot \left(-\frac{t}{\overline{T}_{det}} + 1 \right) \tag{4}$$

where

- t is the time (s)
- $mf_{t=0}$ is the maximum flow of the network (MCM/d) before the failure event
- $\overline{T}_{det}$ is the average detection time (s) which represents the time at which the SCADA communication system closes the pipelines through remote control valves (RCV) when the failure is revealed.

The integral of $g_{deg}(t)$is the robustness capacity model function G_{RobCap}- expressed in m^3- evaluated between 0 and $\overline{T}_{(det)}$as follows:

$$G_{RobCap}\left(\overline{T}_{det}\right) = \int_0^{\overline{T}_{det}} g_{deg}(t)\, dt \tag{5}$$

For simplicity, a linear function is introduced to model the pipeline delivery node pressure degradation over time (Gonzalez De Durana et al., 2014):

$$\frac{dP}{dt} = m \tag{6}$$

The SCADA network detects the pressure decreasing inside the pipeline when it drops by *K*% of the initial value. The final pressure retained in the pipeline depends on the delay of the information from the central SCADA node to the RTUs.

5.3. Gas pipeline network recovery model

The recoverability of a gas pipeline transmission network is here interpretated as the network ability of returning to a normal state after degradation or failure events (Platt, Brown, & Hughes, 2016). When a pipeline fails, through repair, it recovers over time until its nominal capacity is re-gained.

To model the pressure recovery inside a pipeline, for simplicity, we adopted the recovery function explained in (Zhang et al., 2018) as follows:

$$P_{ij}(t) = P_{initial(i,j)} + \left(P_{initial(i,j)} - P_{fin.real(i,j)}\right) \cdot \left(1 - exp\ \left(-\quad b_{ij} \cdot t\right)\right) \tag{7}$$

where $P_{(initial(i,j))}$ and $P_{(fin.real(i,j))}$ are the initial and the real final pressures of the pipeline (i,j) after the degradation phase and b_{ij} is a semi-empirical parameter representing the recovery speed of the pipeline. The problem of Eq. (7) is that we don't have the availability to evaluate b_{ij} in order to estimate the pipeline (i,j) pressure response. By definition of first-order systems, the time constant τ is related to the pipeline recovery speed parameter by the relation $b_{ij} = 1/\tau$. We know, however, that b_{ij}depends, accordingly to empirical observations and hydraulic simulations, on the length of the pipeline under analysis and on the set point pressure $P_{(initial(i,j))}$. The longer the pipeline and the higher the $P_{(initial(i,j))}$ value to reach, the greater the transient will be.

To provide a rough estimate of the value of b_{ij}, we consider Fig. 6 to explain the assumptions.

The two curves in the Figure represent the pressure response according to Eq. (7) and to ideal linear response condition. It is therefore important to analyze the stationary response, when 98% of the set-point pressure is reached.

The two curves show different trends but the stationary condition is the same at the time 4τ. Due to the fact that we don't know enough information to estimate τ, we suppose that when the gas reaches the terminal node *j* at the time t_{dest}, a time of 4τ has elapsed. When the system reaches 4τ, 98% of the system pressure has been recovered.

Fig. 6 suggests that in the case of a shorter pipeline or in the case of a lower set point pressure, the steady state is reached faster. The value of

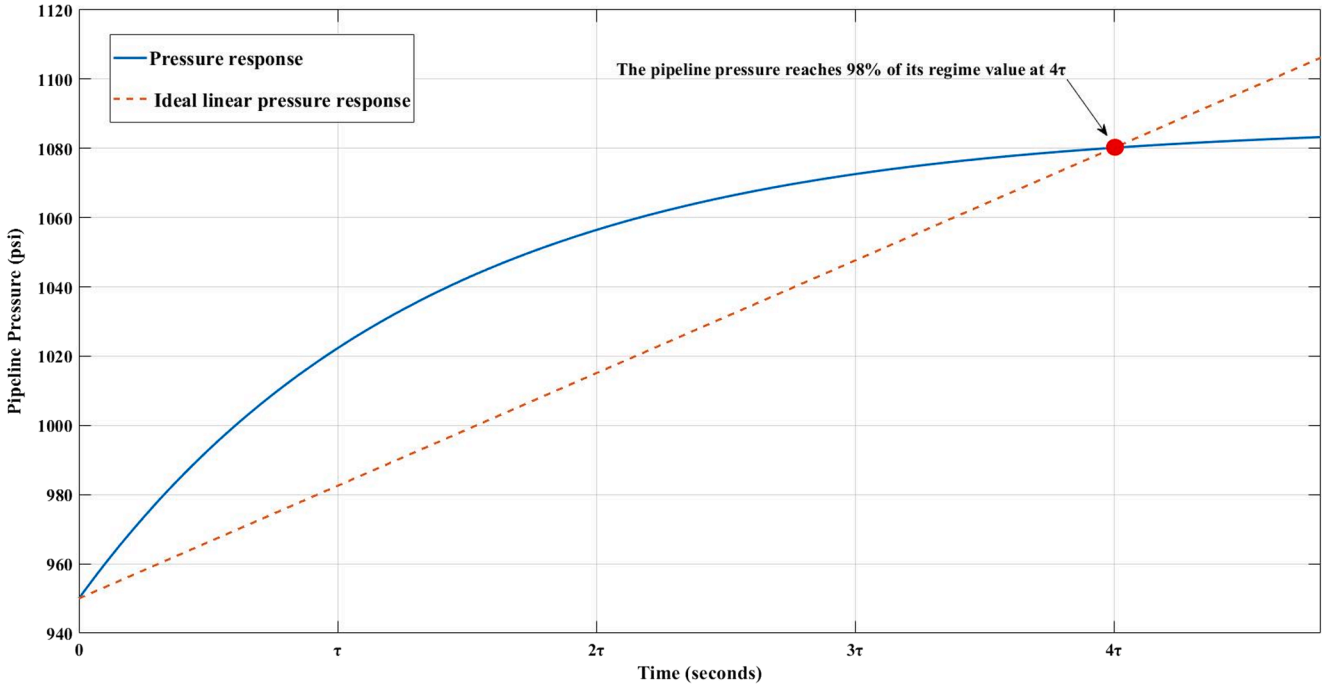

Fig. 6. Pressure response for a generic pipeline. The Figure shows that assuming an ideal linear pressure response with the same regime time 4τ of the real pressure one, the value of $\frac{dP}{dt}$ is an indication of the speed of pressure recovery inside the pipeline.

the time constant τ will take on a lower value while dP/dt for the ideal linear pressure response will be higher due to the upward translation. The dP/dt value for an ideal pressure response provides an estimation of b_{ij}. To semplify the analysis, we assume that after the failure is repaired, the gas is processed inside the involved pipelines at a constant speed (v_{gas}) less than 30 m/s to avoid erosion problems under excessive gas velocity (Neacşu, Suditu, & Stoica, 2013). The value of $t_{dest}$is, then, calculated dividing the pipeline length by (v_{gas}).

The recovery speed parameter b_{ij} for a pipeline (i,j) is, then, calculated as follows:

$$b_{ij} \sim \frac{P_{initial(i,j)} - P_{fin.real(i,j)}}{4\tau} \tag{8}$$

By definition, $P_{(fin.real(i,j))}$ is computed through Eq. (7).

At each time instant t, according to (Zhang et al., 2018), it is assumed that a failed pipeline recovers its transport capacity as follows:

$$Q_{ij}(t) = Q_{ij,0} \cdot \left[1 - exp\left(-\ b_{ij} \cdot t\right)\right] \tag{9}$$

where $Q_{(ij)}(t)$ is the transmission capacity of the pipeline (i,j) at time t, $Q_{(ij,0)}$is the original initial transmission capacity of the pipeline (i,j) before the failure event and b_ij is the recovery speed parameter of the pipeline (i,j).

By rearranging the previous equation we get:

$$Q_{ij}(t) = D_{ij}^{\delta} \cdot \left\{1 - exp\left[-\left(\frac{v_{gas} \cdot \left(K \cdot P_{initial(i,j)} + mpd \cdot m\right)}{L_{ij}}\right) \cdot t\right]\right\} \tag{10}$$

where

- $D_{ij}$is the diameter of the pipeline (i,j) in meters (m)
- δ is an adimensional conversion coefficient for pipeline capacity calculation
- V_{gas} is the recovery gas speed (m/s) at which the gas is processed within the network to recover nominal performance.

The other parameters are the same as explained in Section 5.2.

The area below the recovery function – called $g_{rec}(Q_{ij}(t), t)$- is the network recovery capacity $G_{RecCap}(T_{rec})$, which represents the amount of natural gas processed during the network recovery, expressed in m^3.

G_{RecCap} is defined as follows:

$$G_{RecCap}(T_{rec}) = \int_0^{T_{rec}} g_{rec}\left(Q_{ij}(t), t\right)\, dt \tag{11}$$

where

- t is the time (s)
- $g_{rec}$is the network recovery function, which depends on the capacity of the pipelines at the recovery time t
- T_{rec} is the observation time during recovery (s).

5.4. Resilience performance indices

Robustness and recoverability indices have been developed to quantify the network resilience (Tierney & Bruneau, 2007). These metrics are based on the integration of the area under a resilience function between different time intervals t_1 and t_2.

5.4.1. Network robustness performance index

$$R1 = 1 - \frac{\varphi(t_0) \cdot (t_d - t_e) - \int_{t_e}^{t_d} \varphi(t) dt}{\varphi(t_0) \cdot (t_d - t_e)} \tag{12}$$

R1 provides a percentage of the performance maintained after failure. This performance index identifies the percentage quantity of gas that is supplied in the network despite the failure compared to the maximum capacity.

5.4.2. Network recoverability performance index

$$R2 = 1 - \frac{\varphi(t_f) \cdot (t_f - t_r) - \int_{t_r}^{t_f} \varphi(t) dt}{\varphi(t_0) \cdot (t_d - t_e)} \tag{13}$$

R2 is an index that indicates the percentage quantity of gas that is recovered during the recovery time $T_{rec}$with respect to the quantity of gas that would be supplied if the failure did not occur during the same time T_{rec}.

R2 is "memoryless", in that its value at a given time does not take into account the information before the time at which the recovery starts (Barker, Ramirez-Marquez, & Rocco, 2013).

6. Sensitivity analysis framework

Sensitivity analysis aims to give insights on model behavior, on its structure and on its response to changes in the models inputs (Lloyd et al., 2007; Oakley). In this Section, a sensitivity analysis framework is developed to analyze the resilience model for extracting relevant information, understanding it and eventually supporting decision-making.

6.1. Context

We follow the framework of global sensitivity analysis and assume to have a r-dimensional input random vector $\sigma^* = (X_1, X_2, X_3 \cdots, X_r) \in \mathscr{X}$. A generic function $f: \mathscr{X} \rightarrow \mathscr{Y}$ maps the input space $\mathscr{X} \subseteqq \mathbb{R}^r$ to the output space $\mathscr{Y} \subseteqq \mathbb{R}$. In this work, f is deterministic. The input uncertainty propagates through f, so that the output Y becomes a random variable.

6.2. Analysis of the output distribution

In this work, we consider various statistics including mean and quatiles as a summary of the output distribution (Pete Loucks, 2017, 2017). In general, the α-quantile of a continuous random variable X is defined as the smallest value $q_{(\alpha)}$such that X has a probability α, that is:

$$F_X(q_\alpha) = \alpha = \int_{-\infty}^{q_\alpha} f_X(x)\ \ dx \tag{14}$$

where F_X is the cumulative distribution function (*CDF*) and $f_X(x)$ is the corresponding probability density function (*PDF*) of X (Zio, 2007, 2007).

Frequently reported quantiles are the first, second and third quantiles ($q_{0.25}$, $q_{0.50}$, $q_{0.75}$, respectively). The interquartile range $[q_{0.25}, q_{0.75}]$ provides a quick description of the range of values.

From a practical point of view, in the field of gas pipeline transmission network resilience, it is important to understand the following information: the probability that at a certain time the network has recovered 70, 80 or 90% of its nominal performance and the probability that the network continues to process a certain quantity of gas despite the occurring failure scenario. Such information can be obtained by computing the quantiles of the output distributions.

One of the main objectives of sensitivity analysis is parameter prioritization, which involves the quantification of the influence of each input to the model outputs by sensitivity indices (Morio, 2011).

6.3. Parameter prioritization

In general, sensitivity analysis methods can be classified into local and global (Lv, Tian, Wei, & Xi, 2019). Local sensitivity analysis methods investigate the importance of inputs in a specific area in the input space, whereas global sensitivity analysis methods consider the entire input distribution. In this work, we consider one of the most popular global sensitivity indices, the variance-based sensitivity indices, also called Sobol indices (Sobol, 1993).

6.3.1. Sensitivity indices estimation for single input parameters

Sobol indices rank importance input variables based on their contribution to the model output variance. The main advantage of variance-based sensitivity measures is that they do not impose any hypothesis on the model structure.

The first-order Sobol sensitivity index for the *ith* input is defined as follows (Cariboni et al., 2007; Peterson et al., 2009):

$$\eta_i^2 = \frac{Var[E(Y|X_i)]}{Var[Y]} \tag{15}$$

where $Var[Y]$ is the unconditional variance of the model output Y and $Var[E(Y|X_i)]$ is the variance of the conditional expectation computed fixing X_i (Borgonovo and Plischke, 2016; Borgonovo, 2017; Zio, 2009; Most, 2012).

The total-effect index $\eta_{Tot_i}^2$ accounts for the total contribution of input X_i to the output variation, i.e. its first-order effect plus all higher-order effects (interactions) involving X_i. Two input parameters are said to interact when their effect on Y cannot be expressed as a sum of their single effects.

The total-order sensitivity index for the *ith* input is defined as follows:

$$\eta_{Tot_i}^2 = 1 - \frac{Var\left[E\left(Y\middle|\overrightarrow{X}_{\sim i}\right)\right]}{Var[Y]} \tag{16}$$

where $\overrightarrow{X}_{\sim i}$ represents the vector of the inputs except the *ith* input parameter, so that $Var[E(Y|\overrightarrow{X}_{\sim i})]$ measures the variation in the model output when all inputs vary except X_i.

By definition, $\eta_{Tot_i}^2$ is greater than, or equal to η_i^2 in the case that X_i is not involved in any interaction with other input parameters. The difference $\eta_{Tot_i}^2 - \eta_i^2$ measures how much X_i is involved in interactions. A value $\eta_{Tot_i}^2 = 0$ implies that X_i is non-influential and can be fixed to any value of its distribution, without affecting the variance of the output. The sum of all η_i^2 is equal to 1 for additive models and less than 1 for non-additive models. The difference $1 - \sum_i \eta_i^2$ is an indicator of the presence of interactions in the model.

To adapt variance-based sensitivity measures to the capacity recovery model $G_{RecCap}(T_{rec})$, which is a dynamic model, the sensitivity indices are considered as time dependent, i.e. η_i^2 for each time t_r in observation time interval $[0, T]$; at each time t_r, the unconditional variance $Var[Y(t_r)]$ can be decomposed into two parts:

$$Var\ [Y(t_r)] = Var\ \left[E\left(Y(t_r)\middle|\overrightarrow{X}_{\sim i}\right)\right] + E\left[Var\left(Y(t_r)\middle|\overrightarrow{X}_{\sim i}\right)\right] \tag{17}$$

The first-order sensitivity index η_i^2 for X_i at the time step t_r, is computed as follows:

$$\eta_i^2(t_r) = \frac{Var[E(Y(t_r)|X_i)]}{Var[Y(t_r)]} \tag{18}$$

Similarly, the total-effect index $\eta_{Tot_i}^2$ for X_i at the time step t_r, is computed as follows:

$$\eta_{Tot_i}^2(t_r) = 1 - \frac{Var\left[E\left(Y(t_r)\ \middle|\overrightarrow{X}_{\sim i}\right)\right]}{Var[Y(t_r)]} \tag{19}$$

To assess the importance of an input over a given observation time $[0, T]$, the mean of η_i^2 over $[0, T]$ is considered as:

$$\overline{\eta}_i^2 = \int_0^T \eta_i^2(t_r)\ \ dt_r \tag{20}$$

Similarly, the total-effect sensitivity index is computed as follows:

$$\overline{\eta}_{Tot_i}^2 = \int_0^T \eta_{Tot_i}^2(t_r)\ \ dt_r \tag{21}$$

In practice, the above quantities are approximated by Monte Carlo integrals:

$$\overline{\eta}_i^2 \approx \frac{\sum_{r=1}^{N_T} \eta_i^2(t_r)}{N_T} \tag{22}$$

$$\overline{\eta}_{Tot_i}^2 \approx \frac{\sum_{r=1}^{N_T} \eta_{Tot_i}^2(t_r)}{N_T} \tag{23}$$

where $t_1, t_2, \ldots, t_{N_T}$ constitute an equal-length grid on time interval $[0, T]$ and N_T is the number of sub-intervals inside $[0, T]$

6.3.2. Monte Carlo estimation for the first- and total-order sensitivity indices

The estimation of variance-based sensitivity measures can be challenging. Considering a model output function $Y = f(X_1, X_2) : \mathbb{R}^2 \to \mathbb{R}$ with just two input variables X_1 and X_2, the brute force approach requires N_s^2 model runs where N_s is the sample size of X_1 and X_2 (Saltelli, Tarantola, Campolongo, & Ratto, 2004). To reduce the high computational cost, the authors proposed a method that requires $N_s \cdot (k+2)$ runs, where k is the number of input parameters (Saltelli et al., 2004). This method calculates the sensitivity indices (Eq. (22) and Eq. (23)) at the generic time t_r.

6.3.3. Monte Carlo estimation for groups of input parameters

The definition of the variance-based sensitivity index of one single input parameter is easily extended to the sensitivity index of the group of input parameters considering a group gr_j with W inputs $\overrightarrow{X}_{gr_j} = \left\{X_{j1}, X_{j2}, \cdots, X_{jW}\right\}$. The sensitivity index of the *jth* group of input parameters called the "Closed-order sensitivity index" is computed as follows (Anstett-Collin, Goffart, Mara, & Denis-Vidal, 2015):

$$\eta_{gr_j}^2 = \frac{Var\left[E\left(Y\middle|\overrightarrow{X}_{gr_j}\right)\right]}{Var[Y]} \tag{24}$$

where $Var[Y]$ is the unconditional variance of the model output and $Var[E(Y|\overrightarrow{X}_{gr_j})]$ is named the variance of the conditional expectation computed fixing the parameters related to the *jth* group $\overrightarrow{X}_{gr_j}$, and

$$C_{gr_j} = \begin{bmatrix} x_{r+1}^{(1)} & x_{r+2}^{(1)} & \cdots & x_b^{(1)} & \cdots & x_e^{(1)} & \cdots & x_q^{(1)} & \cdots & x_{2r}^{(1)} \\ x_{r+1}^{(2)} & x_{r+2}^{(2)} & \cdots & x_b^{(2)} & \cdots & x_e^{(2)} & \cdots & x_q^{(2)} & \cdots & x_{2r}^{(2)} \\ \cdots & \cdots & \cdots & \cdots & \cdots & \cdots & \cdots & \cdots & \cdots & \cdots \\ x_{r+1}^{(N_s-1)} & x_{r+2}^{(N_s-1)} & \cdots & x_b^{(N_s-1)} & \cdots & x_e^{(N_s-1)} & \cdots & x_q^{(N_s-1)} & \cdots & x_{2r}^{(N_s-1)} \\ x_{r+1}^{(N_s)} & x_{r+2}^{(N_s)} & \cdots & x_b^{(N_s)} & \cdots & x_e^{(N_s)} & \cdots & x_q^{(N_s)} & \cdots & x_{2r}^{(N_s)} \end{bmatrix} \tag{25}$$

measures the first-order effect of $\overrightarrow{X}_{gr_j}$ on the model output.

The operative estimation scheme for the closed-order sensitivity index is similar to that explained in Section 6.3.2; the columns of the matrix C_i are formed by all columns of B except for the columns related to the group of parameters, which are taken from A.

As an example, let us consider a generic model of N_s input parameters $Y = f(X_1, X_2, \cdots, X_{N_s})$ and a given vector group j of the input parameters $\overrightarrow{X}_{gr_j} = \{X_1, X_2, \cdots, X_b, \cdots, X_e, \cdots X_q, \cdots X_r\}$. The matrix C_{gr_j} is the following:

C_{gr_j} is composed by all the columns of B except the *bth*, *eth* and *qth* columns which are taken from A.

6.4. Trend identification analysis of model outputs

Trend identification allows us to understand:

(1) whether an increase or a decrease in an input leads to an increase or a decrease in the model output;
(2) whether the dependence of the function output is monotonic or not on the parameters;
(3) regional contribution in the uncertainty range (Borgonovo, Lu, Plischke, Rakovec, & Hill, 2017).

The most intuitive method for understanding the trend is partial derivatives. The sign of the partial derivatives of the output function $Y = f(\cdot)$– computed with respect to each input variable - can be used as a sensitivity measure for trend identification and displayed through partial derivative scatterplots (D-scatterplot) (Borgonovo et al., 2017). The partial derivative sensitivity measure is defined as follows:

$$\frac{\partial Y}{\partial x_i} = \lim_{\Delta x_i \to 0} \frac{f(x_1, \ldots, x_{i-1}, x_i + \Delta x_i, x_{i+1} \ldots, x_r) - f(x_1, \ldots, x_{i-1}, x_i, x_{i+1} \ldots, x_r)}{\Delta x_i} \tag{26}$$

In this work, we estimate Eq. (26) by considering $\Delta x_i = \frac{x_i(\max) - x_i(\min)}{N_s}$, where $x_i(\max)$ and $x_i(\min)$ are the maximum and minimum values of X_i. In this work, we set N_s to be large, for the sake of accuracy, equal to 10^6, so that $\Delta x_i = 10^{-6}(x_i(\max) - x_i(\min))$. The partial derivative scatterplot is constructed as follows: first, sample input observations $\left\{\overrightarrow{x}^{(i)}\right\}_{i=1}^{N_s}$ according to the joint input distribution; then, evaluate $\frac{\partial Y}{\partial x_i}$ using Eq. (26) at each $\overrightarrow{x}^{(i)}$ with small variation Δx_i; finally, visualize the estimated partial derivatives $\left.\frac{\partial Y}{\partial x_i}\right|_{\left\{\overrightarrow{x}^{(i)}\right\}_{i=1}^{N_s}}$ along the support of X_i.

For a partial derivative plot, we consider a positive contribution if the point is above and a negative contribution if it is below the value of zero.

6.5. What-if analysis in terms of mean and quantiles

The variability of the output could be so large that further analysis needs to be conducted to investigate the model. For this purpose, a "what-if" analysis (Golfarelli and Rizzi, 2008; Golfarelli et al., 2007) is carried out in order to better understand what happens to the output if the range of parameters uncertainty is reduced.

In this work, we define a new measure to quantify the variation of the output in different failure scenarios. The proposed index borrows the idea from the value of information (Strong Mark Jeremy Oakley, xxxx), and enable focusing on commonly-used statistics like mean and quantiles. Specifically, we define the modified value of information index as:

$$D\left(d_i, d_i'\right) = \frac{I_s\left[Y, d_i'\right] - I_s[Y, d_i]}{I_s[Y, d_i]} \cdot 100\% \tag{27}$$

where I_s denotes the statistics of the output Y sample, e.g. the quantile q; d_i and d_i' are the characteristics of the input distribution in the base and alternative scenarios.

The index $D(d_i, d_i')$ is an indication of how much in percentage an output statistic varies due to an update of information on the input distribution. To estimate Eq. (27), we simulate Y with respect to d_i and d_i', and compute the corrisponding I_s. In this work, we consider mean and quantiles as statistics I_s of the outputs as they provide the information of interest about the output distribution.

7. Case study

7.1. Part 1: Resilience analysis

The developed framework of resilience analysis has been applied to an artificial natural gas transmission network, through the use of network information presented in the reference work (Praks et al., 2015). Gas trasmission network is shown in Fig. 7. In total, there are 4 supply nodes: 2, 10, 11 and 19 (see Table 1). Node number 1 and node number 55 (not reported in the network) are fictitious nodes, specifically the supersource node and the supersink node. The maximum flow of the network is computed using the Ford Fulkerson algorithm. The physical limits of gas sources, capacities of connected elements and node demands are used as constraints for the maximum flow algorithm.

Gas sources information (Table 1), data of pipeline network (Table 2), deterministic customer demands (Table 3), and components failure probabilities are provided. Pipeline capacities and gas demands are expressed in MCM/d (million cubic meters per day).

Transportation capacities of pipelines reported in Table 2 and the demand of the nodes in Table 3 are the same of reference (Praks et al., 2015). Pipeline flows and pressures of the nodes have been calculated with Pipe flow Expert®.

The pressure values reported in Table 4 are estimated assuming:

(A) Source pressure nodes of 75 bar (1087 psi).
(B) Gas methane at the temperature of 293 K, whose density is 7.398 kg/m^3 and viscosity of 0.010 cP.
(C) Carbon Steel pipelines with internal roughness of 0.070 mm.
(D) Using the gas route information provided by Pipe Flow Expert®, 42.66 MCM/d is the network maximum flow found by Matlab® after having constructed the directed weighted graph, whose weights are the values of the pipeline capacities.

Table 5 reports the relevant network components analysis found through the risk matrix model of Section 4.2. Pipelines and compressor station failures give low risk (risk matrix reports values of risk between 1 and 3). The case is different for gas storage and LNG terminal, which have high risk categories.

The network resilience is, then, assessed considering three risk significant scenarios:

(A) Gas storage failure at node 19
(B) LNG terminal failure at node 10
(C) Compressor station shortage due to DDoS black hole attack.
(D) SCADA network was simulated using Network Simulator® and NSG 2.1® as script generator for the first one.

The model of the communication network has been presented in Section 2 and Table 6 reports the empirical SCADA data considered in the simulation. We chosen the UDP protocol and not the TCP based on the assumption that when a packet is loss, it is not necessary to recover that packet but just to know the current state of the pipeline despite the loss of previous information. For the encoding, the CBR (Constant Bit Rate) has been preferred to VBR (Variable Bit Rate) supposing that information packets are sent at regular intervals over time, for simplicity

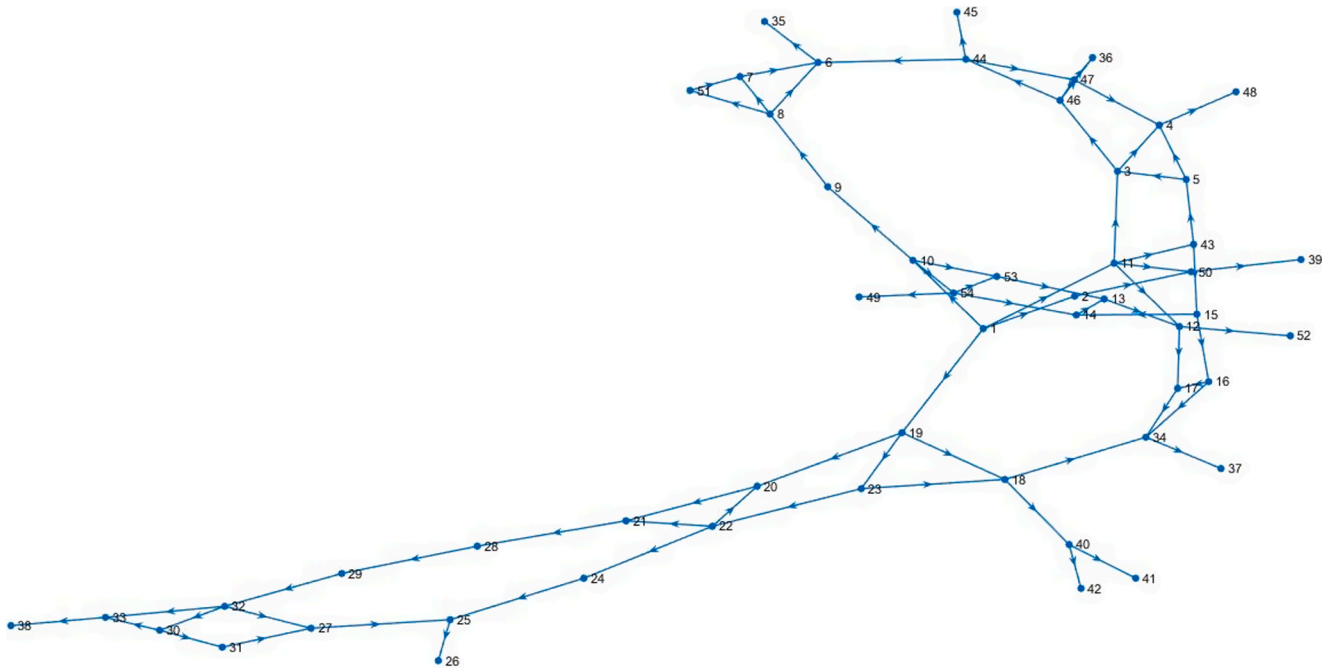

Fig. 7. Layout of the fictious gas transmission network.

Table 1
Properties of the gas network sources.

Gas network node	Type	Limit Capacity (MCM/d)
2	*Immission Source*	31
10	*LNG terminal*	10.5
11	*Immission Source*	7.1
19	*Gas Storage*	25

of modeling. The average and maximum packets delay computed in case of normal functioning are 0.63 and 13.40 s and, under black hole DDOS attack, no information arrives at the SCADA control center starting from the RTUs, due to the absorption of legitimate packages by compromised nodes that act as black holes.

For failure scenarios A and B, Eq. (7) has been applied to obtain the real pressure values retained inside each pipeline involved after the RCVs blocking. For the failure scenario C, instead, the degradation pressure of the pipeline (11, 12) was calculated through the simulation in Pipe Flow Expert® since it is not possible the application of the pipeline pressure degradation model. Inside the pipelines surrounding the compressor station, gas flow continues to be processed and it is not blocked by RCVs.

Eq. (11) was also applied to simulate the delivery node pressure recovery for the failed pipelines of each failure scenario. For the calculation of the recovery speed parameter b, Eq. (9) was used for each pipeline under analysis.

Table 7 reports the results the analysis of the failure scenarios for the assumptions of pressure degradation rate m of 0.577 psi/s and 1 psi/s. Pressure values of the pipelines, SCADA detection times and recovery speed parameters are reported for each failure scenario event.

In the failure scenario A there is more time to detect the fault than in scenario B, because the pressure inside the pipeline reaches the threshold value of −10% of $P_{initial}$in a longer time.

The SCADA detection times for the failure scenario C reports null values, since the SCADA system does not actually have to detect any failures: the operator in the compressor station reduces the gas pumping to safety values to avoid the MAOP achievement. The pipeline (11, 12) is not blocked by the block valve station and the gas continues to flow inside, it even though with a lower flow rate (80%).

To increase the responsiveness of the SCADA system, the threshold for detecting the fault should be reduced to a lower value, e.g. as 8%. This would improve the efficiency of the SCADA system by almost 22%, ensuring a faster recovery.

Robustness and recoverability performance indices were used to quantify network resilience, whose values are reported in Table 8. The recoverability performance index *R2* was evaluated for a recovery time of 20, 60 and 120 s. According to the results of Table 8 it can be observed that the gas pipeline transmission network has a greater robustness to the failure of the LNG terminal than to that of the gas storage. Despite this, the network recovers its starting performance in a shorter time when the gas storage failure occurs rather than that of the LNG: after about 120 s the stationary condition can be considered reached for the first fault event while the second is still recovering. Scenario C is different due to the rapid weakening of the compressor station. The transport capacity of the network collapses instantaneously, albeit at a limited level of 41.24 MCM/d. Due to the dependence of the recoverability index R2 on the observation recovery time T_{rec}, we report in Fig. 8 the trend of the same index for several T_{rec}.

For the failure scenario C, a further analysis was carried out on the MAOP robustness of the network, as explained in Section 4. According to (Pipeline Pressure Limits), 1200 psig is the MAOP of high pressure transmission pipelines.

The pipeline length between the compressor station and the delivery node number 12 is assumed as 23,000 m. Using Pipe Flow Expert®, we computed a gas velocity inside the pipeline of 27.87 m/s. The delivery time is, therefore, 822 s: this time represents the time that operators realize that the natural gas has not reached the destination node. In the event of spilling, a 20% and 100% diameter break in the pipeline was assumed, obtaining outgoing flow rates of 5.54 kg/s and 222 kg/s respectively, in accordance with Eq. (3). In the case of the modeling of a jet fire, it was reasonable to consider a break of the pipeline of 20% of the diameter: the gas burning velocity is then 5.54 kg/s.

The distances calculated by the jet fire that produce significant damage for equipment (12.5 kW/m^2) and for people (2.5 kW/m^2) are 41.12 m and 8.06 m, respectively.

The VCE consequence analysis is developed considering different types of pressure increasing inside the pipeline linked to the compressor station, as said in Section 4.1.

Table 2
Properties of the gas network pipelines.

Starting Node	Destinationnode	Capacity (MCM/d)	Length (km)	Starting node	Destination node	Capacity (MCM/d)	Length (km)
2	50	31	23	18	23	49.16	43
3	4	49.16	0.1	18	34	2.83	43
3	5	12.11	32	18	40	5.05	148
3	11	12.11	29	19	20	12.11	60
3	46	17.13	22	19	23	12.11	0.1
4	5	12.11	32	20	21	49.16	90
4	47	2	22	20	22	12.11	0.1
4	48	12.11	2	21	22	12.11	90
5	43	5.05	5	21	28	12.11	86
6	7	12.11	80	22	23	7	60
6	8	5.05	80	22	24	12.11	86
6	35	5.05	30	24	25	0.83	86
6	44	5.05	11.16	25	26	12.11	46
7	8	49.16	0.1	25	27	49.16	100
7	51	12.11	200	27	31	5.05	0.1
8	9	2.83	25	27	32	5.05	70
8	51	12.11	200	28	29	49.16	50
9	10	2.83	162	29	32	49.16	195
10	53	1.34	144	30	31	5.05	70
10	54	5.05	144	30	32	0.47	0.1
11	12	2	103	30	33	0.47	60
11	43	12.11	34	32	33	2	60
11	50	49.16	31	33	38	5.05	60
12	13	49.16	85	34	37	2.83	200
12	17	49.16	62	36	46	5.05	24
12	52	12.11	10	37	47	5.05	24
13	14	30.6	0.1	39	50	1.34	106
13	53	2	30	40	41	5.05	32
14	15	5.05	85	40	42	12.11	63
14	54	5.05	30	44	45	5.05	1
15	16	12.11	62	44	46	17.13	23
15	43	12.11	132	44	47	2	23
16	17	25	0.1	46	47	49.16	0.1
16	34	4	24	49	54	0.83	40
17	34	12.11	24	53	54	49.16	0.1
18	19	12.11	43				

Table 3
Properties of the customer demand nodes of the gas network.

Demand Node	Customer Demand (MCM/d)	Demand Node	Customer Demand (MCM/d)
5	3.43	33	0.4
6	0.57	34	1
7	0.66	36	1.74
13	1.03	37	1.3
17	0.46	39	1
18	8.4	41	0.4
21	0.54	42	0.5
25	0.6	43	1.06
26	0.8	44	2.82
27	3.5	47	0.68
28	6	48	1.17
30	0.4	52	0.98

Table 9 reports the values of overpressures for different types of compressor station pressure increasing using the Wiekema method. According to (Casal, 2008d), at a distance of 100 m the obtained pressure values would produce only an annoying noise. In the case that structures were present within 100 m, the effects would be worse with the possibility that these are destroyed by the pressure wave generated by the explosion.

Let us assume another scenario event D which concerns the electricity shortage of a thermoelectric power plant which is a large gas user that produce electricity. Assuming the demand node 36 of the network is a thermoelectric power plant, it is interesting to know whether the interruption of electricity due to a physical or possibly cybernetic failure could affect the performance of gas distribution in the transmission network.

Table 4
Results of pressure nodes of the gas transmission network using Pipe Flow Expert®.

Node	Pressure (psi)	Node	Pressure (psi)
2	1087	28	127
3	924	29	125
4	924	30	118
5	924	31	94
6	875	32	118
7	875	33	94
8	875	34	118
9	903	35	875
10	1087	36	877
11	1087	37	203
12	943	38	114
13	944	39	55
14	944	40	982
15	948	41	979
16	943	42	980
17	943	43	965
18	1065	44	877
19	1087	45	877
20	840	46	890
21	807	47	890
22	840	48	924
23	1087	49	965
24	836	50	1087
25	94	51	875
26	90	52	942
27	94	53	965
		54	965

Table 5
Revelant gas network components analysis.

Type	Max flow degradation (MCM/d)	Annual unreliability	MTTF (Years)	Maximum flow performance drop (%)	Risk Value
Pipeline (2,50)	41.32	0.000805	1241.77	3.14	1
Pipeline (10,54)	37.61	0.00504	197.91	11.83	3
Pipeline (19,18)	41.88	0.001505	663.96	1.82	1
Pipeline (19,20)	41.88	0.0021	475.69	1.82	1
Pipeline (19,23)	41.88	$3.5x10^{-7}$	2857142.85	1.82	1
Pipeline (20,21)	41.88	0.00315	316.96	1.82	1
Pipeline (50,39)	41.32	0.00371	269.04	3.14	1
Compressor Station	41.24	0.25	3.476	3.32	3
Gas Storage	17.66	0.10	9.496	58.60	10
LNG Terminal	33.44	0.15	6.153	21.61	9

Table 6
Network Simulator® parameters for SCADA network simulation.

Communication network parameter	Type/value
Total number of nodes	112
Number of RTUs	10
Data Rate	10 Mb
Command Size	500 bytes
Radio Frequency	900 MHz
Transport Layer Protocol	UDP
Traffic Generator	CBR
Sensor Range	250 m
Routing Protocol	AODV
Simulation Time	60 s

By simulating through Pipe Flow Expert® the interruption of natural gas at node 36, the network must adapt the flow direction of some pipelines. The pipelines that reverse their flow are: (3,5), (4,5), (6,7), (6,8) and (36,47). Using the Ford-Fulkerson algorithm to calculate the maximum gas flow in Matlab® of the adapted network, its value doesn't change remaining at 42.66 MCM/d.

Due to the interruption of gas supply due to the thermoelectric plant failure, the pressure of the network nodes increases slightly up to a maximum of 4 bar. Through regulator stations the pressure of the nodes will be decreased up to the value in normal conditions.

7.2. Part 2: Sensitivity analysis

In this Section, the proposed sensitivity analysis framework for the resilience analysis model has been applied to the gas storage failure that it is the worst scenario. Table 10 reports the features of the pipelines involved in the gas storage failure event and Table 11 presents, instead, the input distributions for the resilence model.

The maximum packets delay (*mpd*) value of a segment of pipeline depends on the number of Remote Terminal Units (RTUs) and on the bit rate of the communication channel in the cyber-network. The *mpd* distribution is obtained by performing 200 simulations using the Network Simulator® software. According to measurement theory (Cowan, 2019), the geometrical features of the pipelines, such as their diameters and lengths, are assumed to have a normal distribution, here considering a mean measurement error of 1% and 1.5% respectively, for conservative reasons. For the sake of simplicity, it has been assumed that V_{gas} has a triangular distribution with mode of 27 m/s and a minimum value not less than 20 m/s, to avoid slow recovery of the network performance. A uniform distribution is considered for the remaining parameters.

7.2.1. Analysis of the model output

In this chapter, we mainly study the distribution of the network robustness G_{RobCap} and the network recovery G_{RecCap}. For a general analysis of the network robustness, we conduct 10^6 simulations to approximate the output distributions.

Fig. 9 shows the empirical *PDF* and *CDF* of $G_{RobCap}\left(\overline{T}_{det}\right)$, where $\overline{T}_{det}$ is the avarage detection time calculated for each simulation. Fig. 9 shows that, since the empirical *PDF* of $G_{RobCap}\left(\overline{T}_{det}\right)$ is skewed right

Table 8
Resilience performance indices results for the three types of scenario events considering different times of recovery.

Resilience Performance Index (RPI)	Scenario A Gas Storage Failure	Scenario B LNG Terminal failure	Scenario C Compressor Station Shortage
Robustness (*R1*)	0.7070	0.8919	0
Recoverability (*R2*) [20sec]	0.8655	0.7818	0.8334
Recoverability (*R2*) [60sec]	0.9552	0.8635	0.9126
Recoverability (*R2*) [120sec]	0.9776	0.9148	0.9515

Table 7
Results analysis of degradation pressures, SCADA detection times and recovery speed parameters for pipelines involved in the failure scenarios.

Scenario event	Pipeline involved	$-10\%\ \boldsymbol{P}_{initial}\ (\overline{\boldsymbol{T}}_{det})$ for $m = 0.577$	$-10\%\ \boldsymbol{P}_{initial}\ (\overline{\boldsymbol{T}}_{det})$ for $m = 1$	Recovery speed parameter (b) for $m = 0.577$	Recovery speed parameter (b) for $m = 1$
(A) Gas storage Failure	Pipeline (18,19)	950 psi (198 sec)	945 psi (120 sec)	0.095	0.099
	Pipeline (19,20)	748 psi (159 sec)	743 psi (98 sec)	0.046	0.049
	Pipeline (19,23)	971 psi (200 sec)	966 psi (122 sec)	34.8	36.3
(B) LNG failure	Pipeline (10,9)	805 psi (170 sec)	799 psi (170 sec)	0.018	0.019
	Pipeline (10,53)	860 psi (168 sec)	854 psi (111 sec)	0.022	0.023
	Pipeline (10,54)	860 psi (168 sec)	854 psi (111 sec)	0.022	0.023
(C) Compressor station shortage	Pipeline (11,12)	939 psi (NULL)	939 psi (NULL)	0.001	0.001

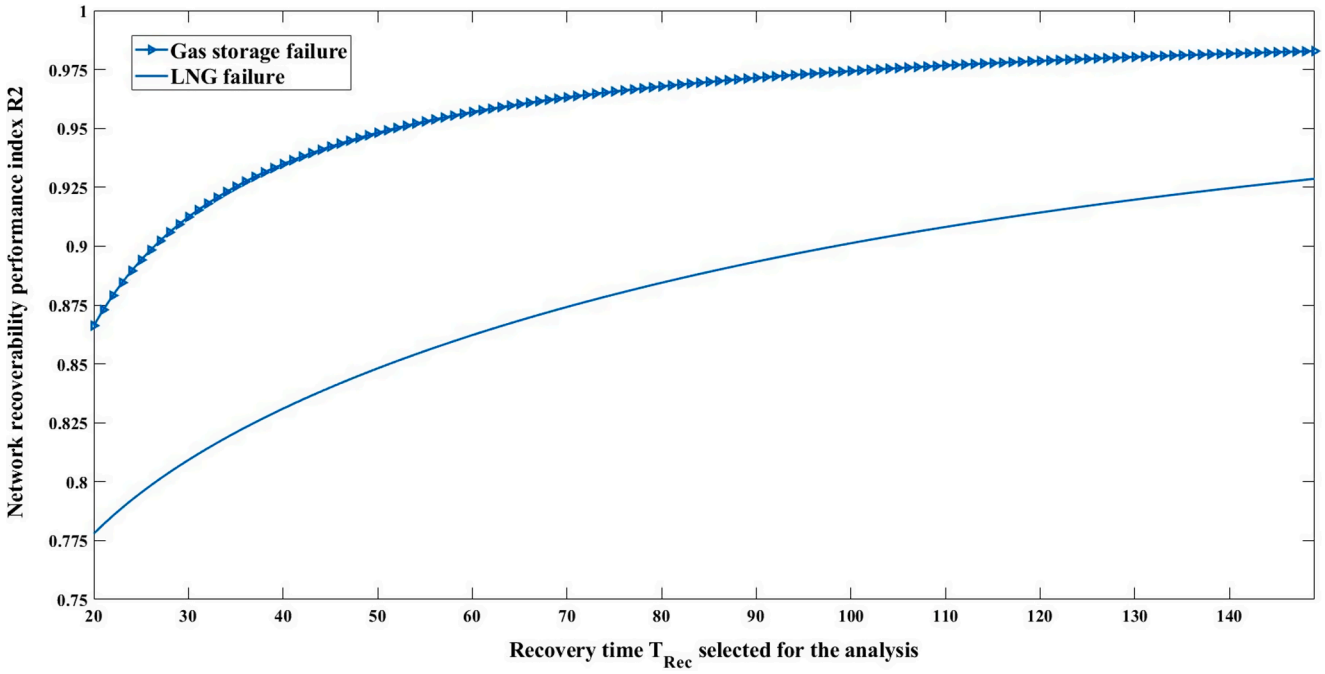

Fig. 8. Network recoverability performance index R2 evolution over time for the failures of gas storage and LNG terminal.

Table 9
Overpressure results for different types of compressor station pressure increasing.

Rate of pressure increase inside the pipeline due to different compressor station response	ΔTime Of spilling (Seconds)	Overpressure (Pa) for $\dot{m} = 5.54$ kg/s	Overpressure (Pa) for $\dot{m} = 222$ kg/s
Linear increase (θ = 0.577)	241	40.1976	137.5565
Linear increase (θ = 1)	209	42.1525	144.2363
Logarithmic increase (λ = 80)	1298	73.8884	252.8467
Logarithmic increase (λ = 90)	83	29.5468	101.1095
Logarithmic increase (λ = 100)	364	48.3636	165.5006

Table 10
Features of the pipelines involved in the gas storage failure.

Pipeline (i,j)	$L_{(i,j)}$ *(m)*	$P_{initial(i,j)}$ *(psi)*	$D_{(i,j)}$ *(m)*
(18,19)	*43,000*	1087	0.768
(19,20)	60,000	840	0.768
(19,23)	100	1087	0.768

significantly, it is interesting to look at the quantiles which are reported in Table 12.

From an engineering point of view, the results in Table 12 and Fig. 9 higlight that the outcome of the degradation process under the input settings in Table 11 possesses large uncertainity, which means that the network ability to resist and absorb can be unstable. With a probability of 0.15, the network robustness is less than $4.4536e+04$ ($q_{0.15} = 4.4536e+04$). The same consideration may be confirmed by the other quantiles. The interquartile ($q_{0.75} - q_{0.25}$) of the gas network robustness $G_{RobCap}\left(\overline{T}_{det}\right)$ is as large as 62759 m^3, showing the extent of the network robustness uncertainity.

$G_{RecCap}(T_{rec})$ is a dynamic function which depends on its observation time T_{rec}. It is not very significant from an engineering perspective

Table 11
Distributions of the input parameters of the resilience model.

Input Parameter	Unit	Type of distribution	Lower value	Upper value
δ	#	Uniform	2.40	2.65
m	Psi/s	Uniform	0.10	1
K	#	Uniform	0.08	0.12
Input Parameter	**Unit**	**Type of distribution**	**Mean μ**	**Standard deviation σ**
Pipeline length *L (i,j)*	m	Normal	*L (i,j)* (Table 10)	0.015 *L(i,j)*
Pinitial (i,j)	psi	Normal	*Pinitial (i,j)* (Table 10)	*0.1 Pinitial (i,j)*
mpd	s	Normal	*12.011*	*1.778*
Diameter D (i, j)	m	Normal	*D (i,j)* (Table 10)	*0.01 D (i,j)*
Input Parameter	**Unit**	**Type of distribution**	**Range**	**Mode**
Vgas	m/s	Triangular	(Goel et al., 2011; Makowski, 2013)	27

studying $G_{RecCap}(T_{rec})$ but it is better to focus on the rate of recovery. In this work, we mainly focus on the beginning and the close-to-end of the recovery process, specifically T_{rec} equals to 5 and 60 s. The network recovery rate is defined as $FR = \frac{Maximum\ \ flow\ \ (T_{rec})}{Maximum\ \ flow\ \ (t=0)}$ where $t = 0$ is the time right before the failure event.

Fig. 10 shows the *PDFs* of the network recovery rate at $T_{rec}$of 5 and 60 s. The shape of the two distributions varies significantly: the *PDF* of $FR(T_{rec} = 60)$ is skewed left at the time 60 s, while the *PDF* of $FR(T_{rec} = 5)$ behaves symmetrically. Fig. 10 shows also that at $T_{rec} = 60$, the network has a larger probability to recover almost 97% of functionality. The difference in the two *PDFs* is that at the initial time the pipelines - previously blocked by the RCVs - will have a much faster transient than the situation at the steady state of 60 s.

The quantile information of $FR(T_{rec} = 5)$ and$FR(T_{rec} = 60)$ are reported in Table 13. The interquartiles ($q_{0.75} - q_{0.25}$) of the gas network recovery $FR(T_{rec} = 5)$ and$FR(T_{rec} = 60)$are as large as 2.89% and 2.11%

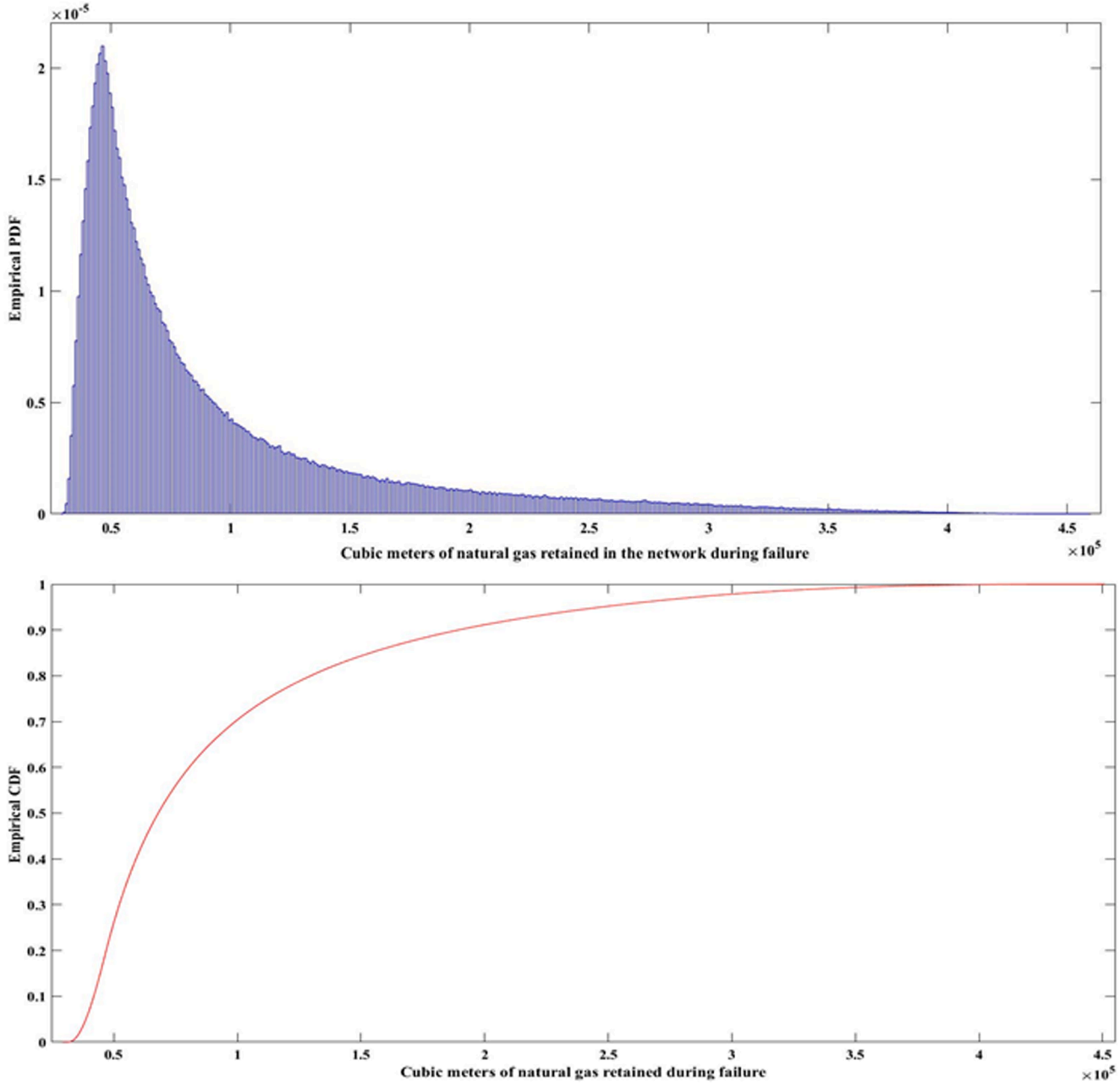

Fig. 9. PDF (top) and CDF (bottom) of the network robustness output $G_{RobCap}(\overline{T}_{det})$ obtained performing 10^6 simulation runs.

Table 12
Mean and quantiles of the empirical PDF of the network robustness $G_{RobCap}(\overline{T}_{det})$.

Statistic of the $G_{RobCap}(\overline{T}_{det})$ *pdf*	Estimation Value (m^3)
$E[G_{RobCap}(\overline{T}_{det})]$	9.4074e+04
$q_{0.15}$	4.4536e+04
$q_{0.25}$	4.9441e+04
$q_{0.50}$	6.7986e+04
$q_{0.75}$	1.1220e+05
$q_{0.90}$	1.8939e+05
$q_{0.975}$	2.9179e+05

respectively, showing small uncertainties for both the recovery times.

The tail distribution that identifies the probability $Pr[FR_{z,t} > FR_Z]$ that at a certain instant time t of the recovery, the network has recovered a level FR_Z of its initial performance is reported in Fig. 11. The Figure shows the probability that the network has recovered 70, 80 and 90% of its original capacity at the generic recovery time t. The probability is almost 1 that the network recovers 70% of its original functionality after around 20 s; the probability of recovering 80% of the initial network capacity grows after 17 s and reaches 1 after 35 s; the network probability to recover to 90% presents a slower trend, reaching a value close to 1 after about 60 s.

7.2.2. *Parameter prioritization analysis*

In this Section, we assess the influence of input parameters onto the uncertainity in the model output, using the variance-based sensitivity measures as explained in Section 6.3. Both individual and group effects are investigated. The communication network input parameters are set

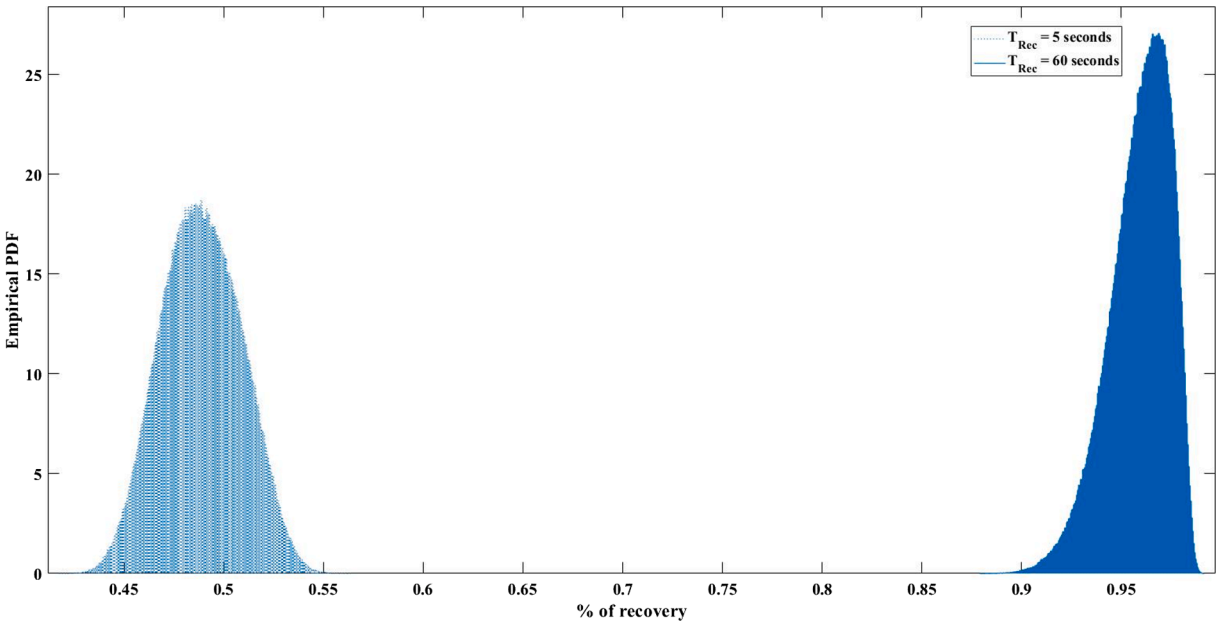

Fig. 10. Probability density functions of the rate of recovery FR at the recovery time of 5 and 60 s.

Table 13
Mean and quantiles of the empirical PDFs of the rate of recovery capacity FR evaluated at the recovery times of 5 and 60 s.

Statistic of the rate of recovery distribution *FR*	Estimation Value (m^3) after T_{rec} of 5 s	Estimation Value (m^3) after T_{rec} of 60 s
$E[FR]$	0.4887	0.9591
$q_{0.15}$	0.4672	0.9430
$q_{0.25}$	0.4742	0.9497
$q_{0.50}$	0.4884	0.9613
$q_{0.75}$	0.5031	0.9708
$q_{0.90}$	0.5154	0.9769
$q_{0.975}$	0.5253	0.9818

to guarantee the network control. For instance, the promptness parameter K is the percentage of the initial pressure that can be detected by SCADA and it is adjustable by network operators. For evaluating the importance of the adjustable communication network parameters, we group them and compute their contribution to the model output variance. The sensitivity indices are estimated via the Monte Carlo-based estimation procedure explained in Section 6.3.2.

7.2.2.1. First-order and total-order effects. Table 14 reports the first-order and total-order sensitivity index results for the robustness model, calculated by 10^6 model runs per input parameter. Results show that the uncertainity in the output of the robustness model is dominated by the degradation pressure rate parameter m. Adopting the difference $\eta^2_{tot_i} - \eta^2_i$ as a measure, one finds little interactions in the robustness model.

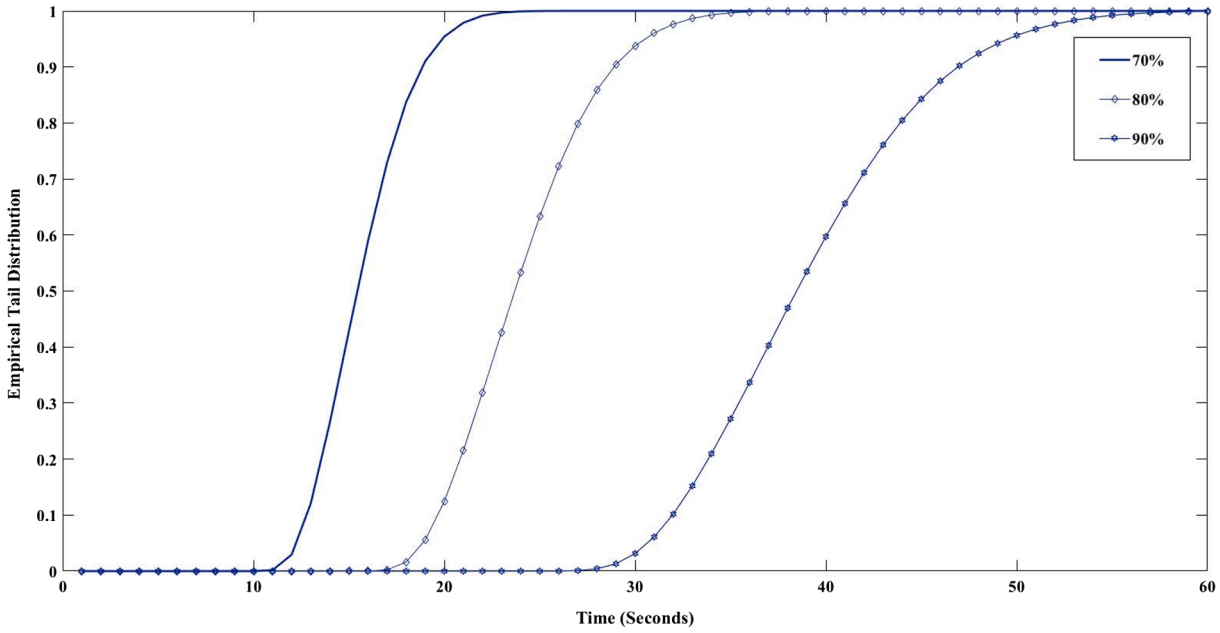

Fig. 11. Empirical tail distribution of the rate of recovery for FR = 70, 80 and 90%.

Table 14
First-order and total-order sensitivity indices of the input parameters of the robustness model.

Robustness model input parameter	$\overline{\eta}_i^2$ (First-order)	$\overline{\eta}_{tot_i}^2$ (Total-order)	$\overline{\eta}_{tot_i}^2$-$\overline{\eta}_i^2$ (Interaction measure)
mpd	0	0.0228	0.0228
Pinitial (18,19)	0.0043	0.0043	0
Pinitial (19,20)	0.0143	0.0143	0
Pinitial (19,23)	0.0040	0.0042	0.0002
m	**0.9588**	**0.9765**	0.0177
δ	0.0027	0.0027	0
K	0.0105	0.0387	0.0282
D (18,19)	0.0036	0.0037	0.0001
D (19,20)	0.0011	0.0011	0
D (19,23)	**0**	**0.0242**	**0.0242**

Table 15
Average first-order and total-order sensitivity indices of the input parameters of the recovery capacity model computed using Eqs. (22) and (23), respectively.

Recovery model input parameter	$\overline{\eta}_i^2$ (First-order)	$\overline{\eta}_{tot_i}^2$ (Total-order)	$\overline{\eta}_{tot_i}^2$-$\overline{\eta}_i^2$ (Interaction measure)
mpd	0.0020	0.0040	0.0020
Pinitial (18,19)	0.0115	0.0157	0.0042
Pinitial (19,20)	0.0179	0.0207	0.0028
Pinitial (19,23)	0.0008	0.0009	0.0001
m	0.0271	0.0312	0.0041
δ	**0.2356**	**0.2450**	0.0094
K	**0.3253**	**0.3291**	0.0038
D (18,19)	0.0410	0.0462	0.0001
D (19,20)	0.0298	0.0310	0.0012
D (19,23)	0.0787	0.0857	0.0070
L (18,19)	0.0008	0.0021	0.0013
L (19,20)	0.0179	0.0207	0.0028
L (19,23)	0.0008	0.0009	0.0001
Vgas	**0.1910**	**0.1920**	**0.0010**

The recovery model – unlike the robustness one – is a dynamic model, whose sensitivity indices vary over time. We report the average sensitivities over a time interval $[0, T = 60]$ and the evolution of the importance of the key drivers over time. Table 15 reports the mean first-order and the mean total-order sensitivity indices of the recovery capacity model obtained with 10^6 samples of each input parameter for each time interval t_r considering $T = 60$ seconds and $N_T = 60$, in Eqs. (22) and (23).

Over the recovery period $[0, T = 60]$, the parameters δ, K and V_{gas} have a significant influence on the uncertainity of the output of the model; in contrast, *mpd* and the lengths of the pipelines have negligible effects. Note that, although m is the most influential parameter for the robustness model, it is much less influential to the recovery model. Network recovery depends little on the speed at which the pipelines have depressurized and much more on the SCADA detection promptness for blocking pipelines through RCVs, which is expressed by the parameter K. Again, the fourth column of Table 15 shows that interaction values have a limited contribution to the network recovery variability.

The analysis of the temporal evolution of the importance of the input parameters is crucial and provides an important insight to understand dynamic models.

Fig. 12 shows the evolution of the first-order sensitivity indices of the most significant parameters over a 60 s observation period ($T_{rec} = 60$ seconds). The total-order sensitivity indices evolution are not reported in this work due to the little interaction values, which make the total-order values similar to those of first-order. One observes that some parameters can be predominant in some moments but less influential in others.

As can be seen from the "horizontal symmetry" of Fig. 12, the importance of δ and diameter D of the pipeline *(19,23)* grows after having touched the minimum approximately after 10 s. V_{gas} and K have the opposite trend than δ and the diameter D of the pipeline *(19,23)* which grows at the beginning and, then, falls. These two parameters reach the same importance after about 43 s. Note that at around 8 s, the four parameters change their behaviors due to the fact that from a mathematical point of view, after the quick transitory, the parameters inside the exponential terms of Eq. (11) become more important than the term D_{ij}^{δ}. The other unshown parameters are almost static, with values close to zero.

Table 16
Closed-order sensitivity indices of groups of parameters of the robustness model.

Group of parameters of the robustness model	η_{gr}^2 (Closed-order)
System Geometry Group	0.0022
Gas Degradation Rate Group	**0.9602**
Communication Network Group	0.0228
Pipeline Pressure Group	0.0034

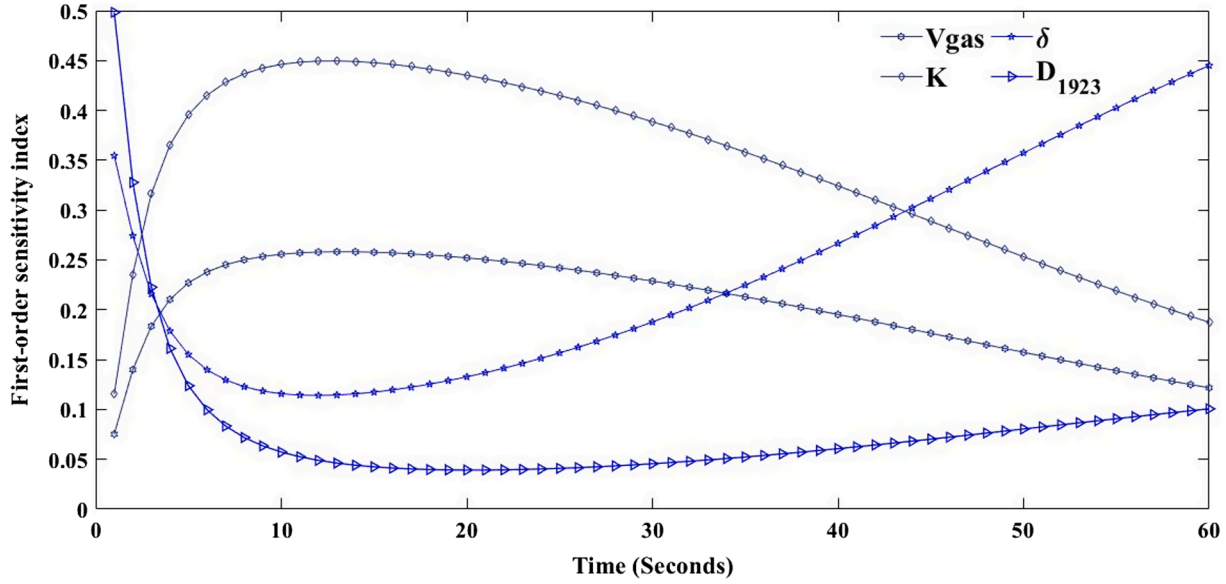

Fig. 12. Recovery capacity model: first-order sensitivity indices of the most important input parameters over 60 s of recovery.

7.2.2.2. Group effects. For the robustness model, we partition the inputs into four groups based on the network features such as the communication network properties, the geometry properties of the pipelines and the pysical properties of the failure event (that is the pressure degradation rate m). In particular the four groups are:

a. System Geometry Group:	*D (18,19), D (19,20), D (19,23),* δ
b. Gas Degradation Rate Group:	*m*
c. SCADA Network Group:	*mpd, K*
d. Pipeline Pressure Group:	*Pinitial (18,19), Pinitial (19,20), Pinitial (19,23)*

The estimated closed-order sensitivity indices for the above groups are shown in Table 16.

The gas degradation rate group consisting of parameter m shows again a clear predominance, contributing to 96% of the variance of output G_{RobCap}. The communication network is slightly more important than the system geometry group and the pipeline pressure group.

The group effect results show that the degradation of a gas pipeline transmission network is a very complex process to manage: the key driver m, unfortunately, is a physical characteristic of the failure that cannot be altered artificially.

The ability of the network to guarantee a good level of performance during a failure depends essentially on the decreasing rate of the pressure inside the pipelines, i.e. the m parameter.

Until the gas reaches the threshold pressure, the SCADA system does not reveal any failure. Even if the performance is degrading, the network continues to process the natural gas until the pipelines are blocked. To further illustrate this concept, suppose having two pipelines that have failed, one with a break of 5% of its diameter and another that has led to a 100% break. In the first pipeline, the pressure will have a much slower decrease than the second one, until it reaches the threshold pressure value and, then, it will be made safe by blocking its sections. This confirms the difficult controllability of the process.

For the recovery model, we consider the following groups:

a. System Geometry Group:	*D(18,19), D(19,20), D (19,23),* δ, *L(18,19),L(19,20), L (19,23)*
b. Gas Rate Properties Group:	m, V_{gas}
c. SCADA Network Group:	*mpd, K*
d. Pipeline Pressure Group:	*Pinitial (18,19), Pinitial (19,20), Pinitial (19,23)*

Table 17 shows the corresponding closed-order sensitivity indices for the recovery model.

The geometry of the pipelines contributes almost to 40% of the output variance, with $\eta^2_{gr}(geom.charact.) = 0.4187$, which is much more than that of the robustness model. The geometric characteristics, such as the pipeline length, play an important role in the recovery: the longer the pipeline, the slower the recovery. The communication network, instead, contributes to almost 32% of the output variance with $\eta^2_{gr}(SCADA) = 0.3241$. Thanks to the possibility of controlling the communication parameter settings, whose closed-order index registers a value of 0.3241, the network recovery turned out to be a more manageable process than the degradation process.

7.2.3. Trend identification

Trend identification analysis is performed to understand whether the key drivers (m for the robustness model and K and δ for the recovery model) found in the parameter prioritization stage have positive or negative effect on the model outputs.

Table 17
Closed-order sensitivity indices of group of parameters of the recovery model.

Group of parameters of the recovery model	η^2_{gr} (Closed-order)
System Geometry Group	0.4187
Gas Rate Properties Group	0.2501
Communication Network Group	0.3241
Pipeline Pressure Group	0.0151

Fig. 13 displays the partial derivative scatterplot (Section 6.4) of the m parameter for the robustness model, where each point represents one of the estimated $\frac{\partial Y}{\partial x_i}$ using Eq. (26) with Δx_i equal to 10^{-6} of the range of m parameter values. Fig. 13 shows that m always has negative effect to the robustness capacity, implying that if the pressure degradation rate increases, the robustness model output decreases; especially, the values between 0.1 and 0.3 psi/s generate strong effect, being associated with larger absolute partial derivatives.

Scatterplots of Fig. 14 and Fig. 15 report the trend identification analysis of parameters K and δ, for the recovery model, at the times of 5 and 60 s, respectively. Fig. 14 shows that parameter K has positive effect on the model output at both times, meaning that if the promptness of the SCADA communication network decreases – caused by an increase of the K parameter - the recovery model output increases both for T_{rec} of 5 and 60 s.

It should not be confused that increasing the promptness of the SCADA system also increases the amount of gas recovered. If the recovery rate increases, the amount of recovery, instead, decreases due to a higher pressure retained in the pipelines. The computed positive partial derivative of $G_{RecCap}(T_{rec})$ with respect to K decreases much quicker at 60 than at 5 s.

Fig. 15 shows that an increase in the δ parameter, will lead instead to a decrease in the quantity of gas processed in the recovery phase, both for T_{rec} of 5 and 60 s.

Recall that δ is a mathematical parameter that allows to calculate the transport capacity of a pipeline knowing its diameter. If this parameter increases, the pipeline capacity also increases (see Eq. (10)) and the network achieves the nominal performance faster than if the pipeline capacity were lower causing a less amount of natural gas recovered due to an overestimation of the initial pipeline capacities.

7.2.4. "What-if" analysis

To understand to what extent the resilience of the network changes if there is a reduction of the uncertainty interval of the key uncertainty drivers, a "what-if" scenario analysis is conducted. From an engineering point of view, the "what-if" analysis results offer practical information to the operation managers.

From the previous analysis, we know that the m parameter is a key driver for the robustness capacity G_{RobCap} of the network. The "what-if" analysis is, then, performed by reducing the uncertainty in parameter m, while keeping its mean as the same.

Considering the robustness model, the different assumptions of the support range of the pressure degradation rate parameter m could lead to take an operational decision over another one. Reduction in the range of support of m simulates the situation that network operators attribute different assumptions to the pressure degradation rate, leading to various G_{RobCap} estimations. Specifically, in the base scenario, we have $m\ u(0.1, 1)$; then, consider an alternative scenario $m\ u(0.145, 0.955)$, where each end of the range is reduced by 5% compared to the base interval $(0.1, 1)$ keeping the same mean. In latter case, the mean of G_{RobCap} has a value of $D(d, d')$ equal to −3.572%. The meaning of this value is that the mean of G_{RobCap} decreases its value respect with the mean of the base scenario where $m\ u(0.1, 1)$.

If another operator considers each end of the range of m reduced by 10% and 20%, i.e., $m\ u(0.190, 0.910)$ and $m\ u(0.280, 0.820)$, the mean of G_{RobCap} assumes a value $D(d, d')$ of −5.9070% and −8.8777% for d' equal to 10% and 20%, respectively.

Fig. 16 shows changes of G_{RobCap} in distribution when considering different case scenarios. Starting with the base scenario, the variance of the robustness capacity G_{RobCap} decreases from $3.32{\cdot}10^7$ to $1.76{\cdot}10^7$, $1.045{\cdot}10^7$ and $4.23{\cdot}10^6$, for d' equal to 5%, 10% and 20%, respectively.

Let us consider the quantile $q_{0.15}$ for the different knowledge of the range of support of m for $m\ u(0.1, 1)$ and for d' equal to 5%, 10% and 20%. The quantile $q_{0.15}$ assumes the values of 4.4536 + 04 m^3 for

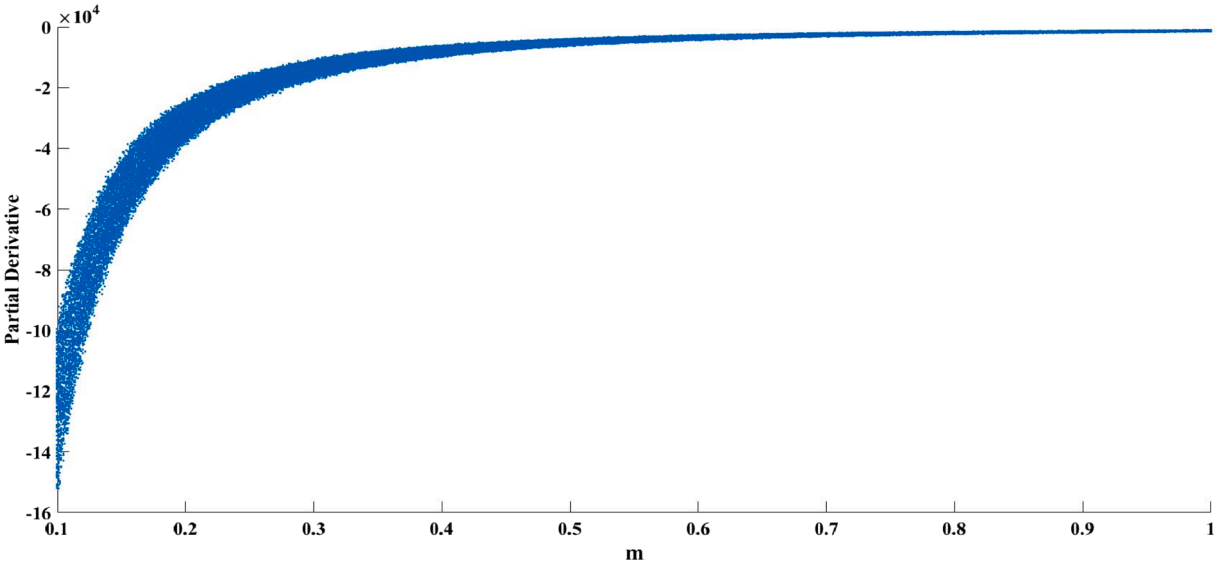

Fig. 13. Trend evolution analysis of the m parameter for the robustness model.

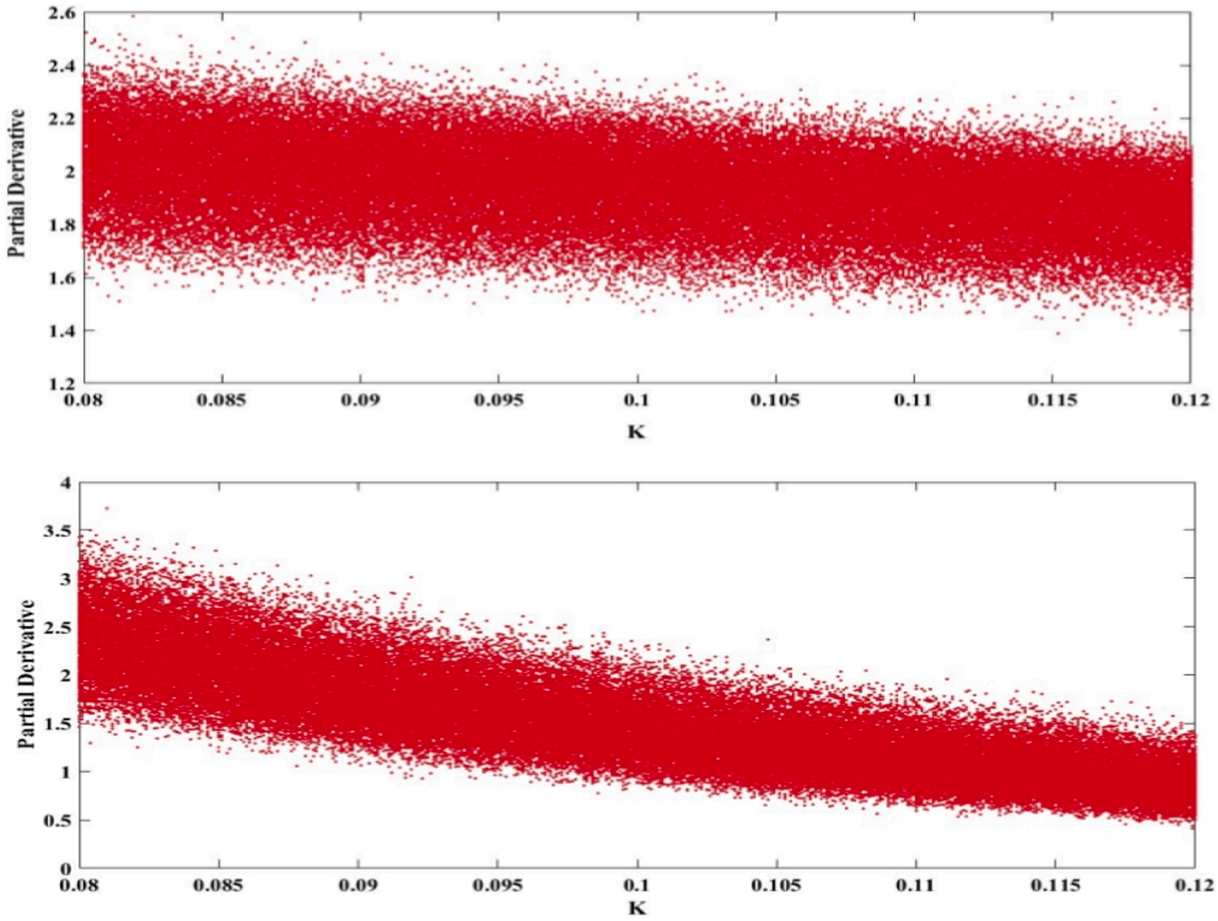

Fig. 14. Trend identification scatterplots for the K parameter at the recovery time of 5 (above) and 60 (below) seconds, respectively.

$m\ u(0.1, 1)$ and $5.1635e+04\ m^3$, $5.1972e+04\ m^3$, $5.2615e+04\ m^3$ for $m\ u(0.145, 0.955)$, $m\ u(0.190, 0.910)$ and $m\ u(0.280, 0.820)$, respectively. The quantile $q_{0.15}$ expresses the probability of 0.85 that, considering a determined range of m, the network is still able to process at least the corrisponding level of natural gas during the degradation process accordingly with the definition of tail distribution $(1 - F_X(q_\alpha) = 1 - q_\alpha)$.

The quantiles values explain that if the uncertainity range of m reduces, keeping the same mean value, the forecast of the natural gas processed in the network despite the gas storage failure increases.

To satisfy the gas demand of the network when gas storage fails, due to equipment failure or to the fact that it is empty, it is necessary to supply the natural gas to the demand nodes exploiting the other gas

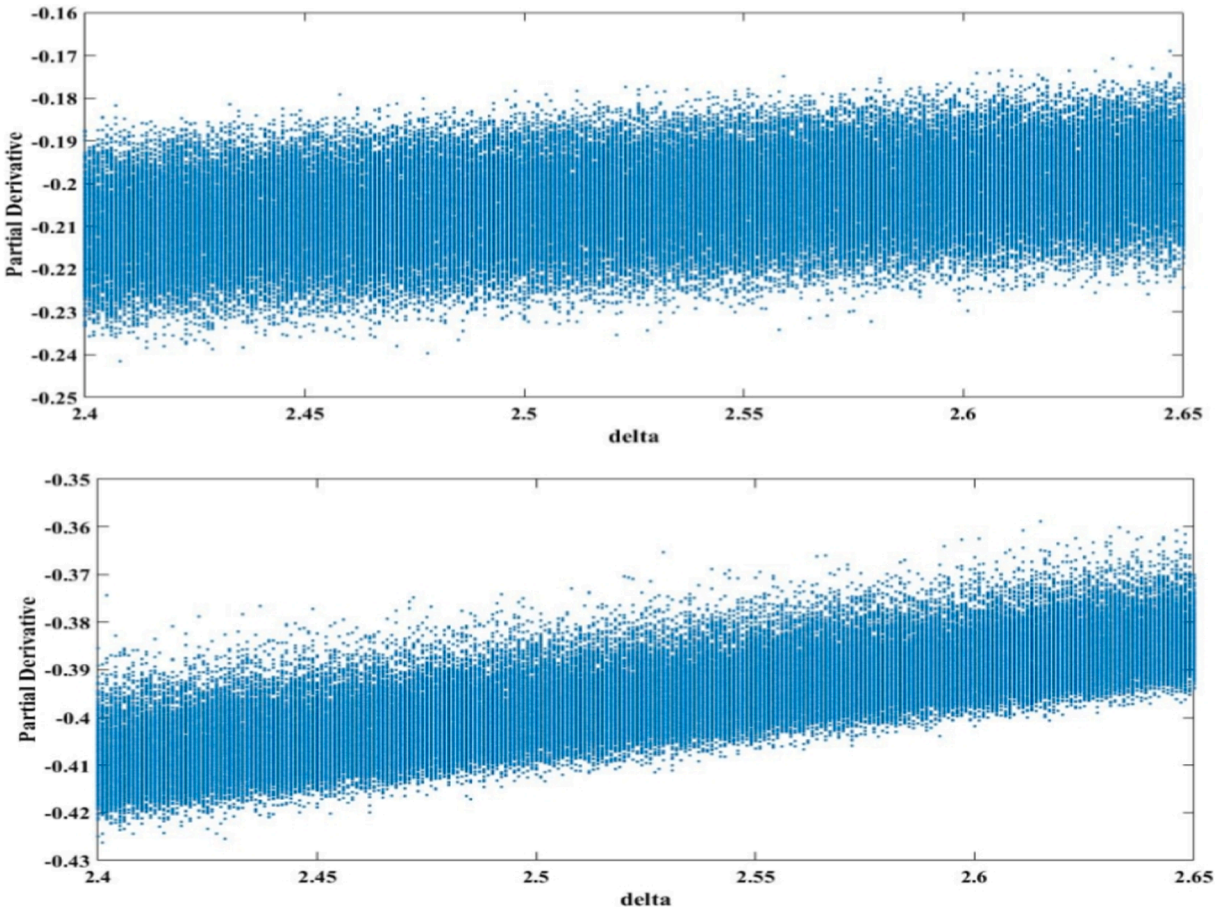

Fig. 15. Trend identification scatterplots for the δ parameter at the recovery time of 5 (above) and 60 (below) seconds, respectively.

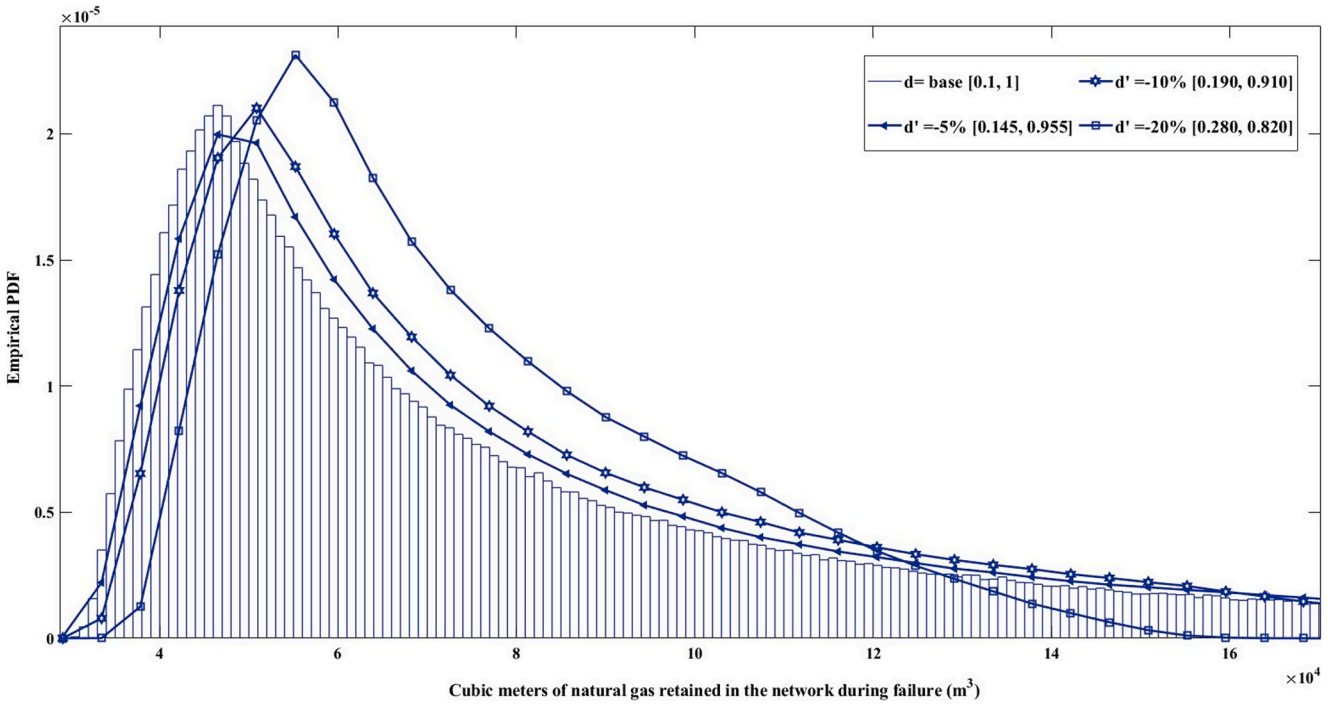

Fig. 16. Variation of the PDF of the robustness model for d' equals to −5,-10 and −20% of the m parameter range.

sources for ensuring the maximum level of satisfaction of the network demand.

Considering the daily demand of the network (see Table 3) of 39.43 MCM/d, we want to analyze the economic loss during the degradation phase to evaluate the possibility to increase the natural gas imported from other countries. Comparing the costs of the partial loss of the demand with those of a possible increase of the natural gas supply from abroad, makes it possible to take accurate decisions to limit any eventual losses. To estimate the costs and the steady gas demand during the degradation process, it is necessary to consider the failure detection time $\overline{T}_{det}$ extracted from Eq. (3) for each different choice of the uncertainity range of m. The quantile $q_{0.15}$ of the output G_{RobCap}, for a conservative reason, is a measure of the amount of natural gas that the network continues to process during the failure event. Table 18 shows the network demand not satisfied, the relative economic loss (€) and the failure detection time $\overline{T}_{det}$for each uncertainty range of m. For this analysis we considered a reasonably natural gas cost for a customer use of 0.85€/m^3. The gas demand not satisfied is computed as the difference between the gas network demand during $\overline{T}_{det}$ and the amount of natural gas processed in the network (the quantile $q_{0.15}$) despite the failure.

Considering a wholesale price of the natural gas of 148 €/*kcm* (Egging, Gabriel, Holz, & Zhuang, 2008) where *kcm* is the notation of "thousands of cubic meters", Table 19 shows the relative costs to be faced to avoid the loss of gas supply to network customers when gas storage facilities fail and the pipelines have not been blocked yet by the SCADA system. The analysis highlights how the increase of the contractual amount of natural gas from other countries it is an advantageous choice in terms of economic terms.

In the same way, different knowldge of the support range of K could lead to different forecasts of the amount of natural gas recovered during the recovery time T_{rec}. Decreasing the support range of K, mantaining the same mean value, implies to increase the accuracy of the measurments by the instrumantation involved in the detection of the pressure at which the pipelines are blocked by RCVs. From the values $D(d, d^{'})$of the quantile $q_{0.90}$ of K, increasing the accuracy of the instrumentation choosing the best pressure sensors, leads to slighly better forcast of the amount of natural gas processed during the recovery phase. One can deduce that increasing the accuracy of the instrumentation does not involve significant forecast changes of the natural gas recovered during the recovery phase.

Due the fact that δ is a mathematical parameter that allows to compute the network pipeline capacities knowing the respective diameters, it is not possible to get engineering practice considerations. In spite of everything, it is however possible to affirm that by restricting the range of δ, mantaining the same mean value, there is a slight improvement in the forecast of the gas recovered during the recovery phase. In other words, different knowledge of the pipeline capacities, restricting the uncertainity range of δ, is irrelevant for engineering forecasts.

8. Conclusions

Nowadays the vulnerability of critical infrastructures has led to the development of frameworks for resilience analysis, including both physical and cyber risks. In this work, we have developed an integrated framework to analyze the resilience of gas pipeline transmission networks.

Appropriate RPIs are provided to assess the resilience of the gas transmission network and to indicate to the system designers and operators, ways to increase the robustness and recoverability of their networks by taking appropriate precautions in the event of cyber-attacks and physical failures. Pressure integrity attacks have been considered due to the great threat of cyber attacks in the Oil & Gas sector, providing an integrated view by analyzing the possible failure events and their impact on the gas network resilience.

An original framework for resilience analysis has been proposed that combines different mathematical and simulation models to capture the complexity of the gas pipeline networks, especially the complex SCADA communication network functioning and structure.

The application of the integrated resilience framework on a resilistic case study higlights how the gas pipeline transmission network is vulnerable to the failure of the gas storage but has a good robustness to that of the LNG terminal.

The recoverability of the network instead, has an opposite trend. The network recovers its initial performance faster when a gas storage failure occurs rather than when it occurs at the LNG terminal, as can be observed by the trend of the network recoverability index performance *R2*.

Furthermore, a novel sensitivity analysis framework for the resilience model of gas pipeline transmission networks has been proposed, to provide comprehensive insights of the complex critical infrastructure for decision-making.

Model output analysis, parameter prioritization, trend identification and a what-if analysis in terms of mean and quantiles have been performed. Due to the time dependence of the recovery model, a conceptual readjustment of the individual and group variance-based sensitivity indices has been necessary.

In the case study considered, the model output analysis results of the tail distribution show that the gas pipeline transmission network recovers 70% of its initial performance very quickly and after 60 s the probability to recover up to 90% is almost 1.

Besides, the sensitivity indices for the pressure degradation rate parameter have pointed out that the degradation of a natural gas transmission network is not easily manageable due to its highly dependence on the speed at which the pressure decreases within the pipelines.

Furthermore, network recovery is a process that can be sped up if good pressurization by RCVs is guaranteed. The individual effect of the K parameter - which represents the promptness of the SCADA system – highlights that the recovery is highly conditioned by this parameter. An increase in the value of K leads to a slow recovery, with a greater quantity of gas being recovered in this phase. The trend identification analysis has discovered the negative effect of the δ parameter during all the recovery phase and points out that overestimating the pipeline

Table 18
Cost analysis considering different assumptions of the uncertainty range parameter m.

Uncertainty range of m	$\overline{T}_{det}$(min)	Gas demand not satisfied (m^3)	Cost related to the gas demand not satisfied (€)
m $u(0.1, 1)$	2.165	14,741	12,530
m $u(0.145, 0.955)$	2.465	15,518	13,190
m $u(0.190, 0.910)$	2.481	15,957	13,564
m $u(0.280, 0.820)$	2.512	16,163	13,739

Table 19
Convenience analysis of purchasing gas from other countries, considering different assumptions of the uncertainty range parameter m.

Uncertainty range of m	Amount of natural gas needed to avoid economic losses (m^3)	Cost related to the eventual gas demand not satisfied (€)	Cost related to the gas purchased from other countries to avoid economic losses (€)	Convenience of purchasing gas from other countries (€)
m $u(0.1, 1)$	14,741	12,530	2182	+10348
m $u(0.145, 0.955)$	15,518	13,190	2297	+10893
m $u(0.190, 0.910)$	15,957	13,564	2362	+11202
m $u(0.280, 0.820)$	16,163	13,739	2392	+11347

capacities leads to an underestimation of the amount of natural gas recovered.

The "what-if" analysis of the robustness model highlights the changes in the output distribution when knowledge of inputs improves, providing additional information to the network owners. The results show that, due to the high dependence of the output on the degradation rate parameter m, the statistics of the network robustness capacity G_{RobCap} vary rapidly if the uncertainty range of m is reduced from 5% to 20% of the initial uncertainty range.

The same analysis on the recovery model, shows a small variability of the statistics of G_{RecCap} if different assumptions are made on the uncertainty range of the parameters K and δ.

It has been highlighted how the "what-if" analysis has great relevance from the engineering point of (Cavallaro et al., 2014) view. Different knowledge of the parameter m relating to the degradation rate, can lead to different decisions on the supply of gas from other countries sources. A correct identification of the range of support of the variability of the m parameter allows to better manage the network resources by the operators during the degradation process, satisfying the demand of the network as much as possible.

At the end of this work, we conclude that:

- The framework proposed to quantify resilience of gas pipeline transmission networks is flexible, adaptable to any complex gas network regardless of the number of nodes and pipelines thanks to the low computational cost of the maximum flow algorithm implemented in Matlab®.
- The resilience analysis framework can be extended for any network degradation and recovery function. Several simplifying hypotheses have been made in this work to facilitate the calculation of the network robustness. More accurate simulations on pipeline depressurization would allow more accurate results on network resilience to specific failures.
- The interdependence model for complex gas networks proposed, although it is only at the first stage, offered results in agreement with the practice. In particular, the model confirms that the degradation process depends very little on the SCADA network settings and very much on the characteristics of the failure. Furthermore, the ability to recover the network, through a bottom-up approach, depends on the time required to bring the pressure of the pipelines to a steady state.
- The Monte Carlo-based algorithm of the sensitivity analysis framework has a low computational cost that allows us to adopt a resilience model with many input parameters considering 10^6 resilience model runs to compute the Sobol's sensitivity indices.
- The "what-if" analysis, included in the four stages of the sensitivity analysis framework, demonstrated the importance of sensitivity analysis in the decision-making process.
- The method of estimating the Sobol sensitivity indices of the first-order and the total-order for the network recovery model can also be extended to other dynamic models. Thanks to the low computational cost of the algorithm proposed for estimating the indices, based on the Monte Carlo method, this work aims to provide support for the sensitivity analysis of dynamic models, a topic little developed in literature.

CRediT authorship contribution statement

Antonio Marino: Writing – original draft, Methodology, Software. **Enrico Zio:** Writing – review & editing, Supervision.

Declaration of Competing Interest

The authors declare that they have no known competing financial interests or personal relationships that could have appeared to influence the work reported in this paper.

Acknowledgement

None.

References

Abrams, M., & Weiss, J. (2008). *Malicious control system cyber security attack case study – Maroochy Water Services, Australia*. MITRE.

Anstett-Collin, F., Goffart, J., Mara, T., & Denis-Vidal, L. (2015). Sensitivity analysis of complex models: Coping with dynamic and static inputs. *Reliability Engineering & System Safety, 96*, 440–449.

Attoh-Okine, N. O. (2016). *Resilience engineering: Models and analysis* (pp. 11–22). Cambridge University Press.

Barker, K., Ramirez-Marquez, J. E., & Rocco, C. M. (2013). Resilience-based network component importance measures. *Reliability Engineering & System Safety, 117*, 89–97.

Borgonovo, E. (2017). Global sensitivity analysis. *International Series in Operations Research and Management Science*.

Borgonovo, E., Lu, X., Plischke, E., Rakovec, O., & Hill, M. C. (2017). Making the most out of a hydrological model data set: Sensitivity analyses to open the model black-box. *Water Resources Research, 53*(9), 7933–7950. https://doi.org/10.1002/2017WR020767

Borgonovo, E., Lu, X., Plischke, E., Rakovec, O., & Hill, M. C. (2017). Making the most out of a hydrological model data set: Sensitivity analyses to open the model black-box. *Water Resources Research, 53*(9), 7933–7950. https://doi.org/10.1002/2017WR020767

Borgonovo, E., & Plischke, E. (2016). Sensitivity analysis: A review of recent advances. *European Journal of Operational Research, 248*(3), 869–887.

Cariboni, J., Gatelli, D., Liska, R., & Saltelli, A. (2007). The role of sensitivity analysis in ecological modelling. *Ecological Modelling, 203*(1-2), 167–182.

Cariboni, J., Gatelli, D., Liska, R., & Saltelli, A. (2007). The role of sensitivity analysis in ecological modelling. *Ecological Modelling, 203*(1-2), 167–182.

Carvalho, R., Buzna, L., Bono, F., Gutiérrez, E., Just, W., & Arrowsmith, D. (2009). Robustness of trans-European gas networks. *Physical Review. E, Statistical, Nonlinear, and Soft Matter Physics, 80*(1). https://doi.org/10.1103/PhysRevE.80.016106

Casal, J. (2008a). Evaluation of the effects and consequences of major accidents in industrial plants. *Industrial Safety Series, 8*, 90–98.

Casal, J. (2008b). Evaluation of the effects and consequences of major accidents in industrial plants. *Industrial Safety Series, 8*, 120–135.

Casal, J. (2008c). *Evaluation of the effects and consequences of major accidents in industrial plants* (vol. 8,, 30–33.

Casal, J. (2008d). Evaluation of the effects and consequences of major accidents in industrial plants. *Industrial*, 270.

Cavallaro, M., Asprone, D., Latora, V., Manfredi, G., & Nicosia, V. (2014). Assessment of Urban Ecosystem Resilience through Hybrid Social-Physical Complex Networks. *Computer-Aided Civil and Infrastructure Engineering*. https://doi.org/10.1111/mice:12080

Chai, W. K., Kyritsis, V., Katsaros, K. V., & Pavlou, G. (2016). Resilience of interdependent communication and power distribution networks against cascading failures. *2016 IFIP Networking Conference (IFIP Networking) and Workshops, IFIP Networking 2016*.

Chopade, P., & Bikdash, M. (2012). Modeling for survivability of smart power grid when subject to severe emergencies and vulnerability. *Conference Proceedings – IEEE SOUTHEASTCON*.

Cowan, G. (2019). Statistical models with uncertain error parameters. *European Physical Journal C*.

di Maio, F., Nicola, G., Zio, E., & Yu, Y. (2014). Sensitivity Analysis and Failure Damage Domain Identification of the Passive Containment Cooling System of an AP1000 Nuclear Reactor. hal-01787161. *Probabilistic Safety Assessment and Management Conference, 2014, Honolulu, United States*.

Di Maio, Francesco, Picoco, Claudia, Zio, Enrico, & Rychkov, Valentin (2017). Safety margin sensitivity analysis for model selection in nuclear power plant probabilistic safety assessment. In *Reliability Engineering and System Safety, 162* pp. 122–138). Elsevier. https://doi.org/10.1016/j.ress.2017.01.020ff. ffhal-01652238f.

Ebrahimy, R. (2014). Investigating SCADA Failures in Interdependent Critical Infrastructure Systems. arXiv Prepr. arXiv1404.7565.

Egging, R., Gabriel, S. A., Holz, F., & Zhuang, J. (2008). A complementarity model for the European natural gas market. *Energy Policy, 36*(7), 2385–2414.

EGIG. (2011). *Gas Pipeline Incidents: 8th Report of the European Gas Pipeline Incident Data Group*. EGIG.

Fall, K., & Varadhan, K. (2011). The ns Manual (formerly ns Notes and Documentation). *The VINT Project*.

Filippini, R., & Silva, A. (2014). A modeling framework for the resilience analysis of networked systems-of-systems based on functional dependencies. *Reliability Engineering & System Safety, 125*, 82–91.

Ganguly, A. R., Bhatia, U., & Flynn, S. E. (2018). Critical Infrastructures Resilience. pp. 41–43.

Ganguly, A. R., Bhatia, U., & Flynn, S. E. (2018). Critical Infrastructures Resilience. pp. 90–93.

Gao, J., Liu, X., Li, D., & Havlin, S. (2015). Recent progress on the resilience of complex networks. *Energies, 8*(10), 12187–12210.

Gas Pressure Regulation and Overpressure Protection. [Online]. Available: http://puc.sd.gov/commission/PSOT/Presentation/regulatoroverview.pdf.

Goel, S., Aggarwal, V., Yener, A., & Calderbank, A. R. (2011). The effect of eavesdroppers on network connectivity: A secrecy graph approach. *IEEE Transactions on Information Forensics and Security, 6*(3), 712–724.
Golfarelli, M., Rizzi, S., & Proli, A. (2007). Designing what-if analysis.
Golfarelli, M., & Rizzi, S. (2008). UML-based modeling for what-if analysis. *Lecture Notes in Computer Science (including subseries Lecture Notes in Artificial Intelligence and Lecture Notes in Bioinformatics)*.
Gonzalez De Durana, J. M., Barambones, O., Kremers, E., & Varga, L. (2014). Agent based modeling of energy networks. *Energy Conversion and Management, 82*, 308–319.
Grossel, S. S. (2001). Guidelines for chemical process quantitative risk analysis. *Journal of Loss Prevention in the Process Industries, 14*(5), 438–439.
Henry, D., & Ramirez-Marquez, J. E. (2012). Generic metrics and quantitative approaches for system resilience as a function of time. *Reliability Engineering & System Safety, 99*, 114–122.
Hildick-Smith, A. (2005). Security for critical infrastructure scada systems. *SANS Read. Room, GSEC Pract. Assignment*.
Homma, T., & Saltelli, A. (1996). Importance measures in global sensitivity analysis of nonlinear models. *Reliability Engineering & System Safety, 52*, 1–17.
Hu, Y., Ksherim, B., Cohen, R., & Havlin, S. (2011). Percolation in interdependent and interconnected networks: Abrupt change from second- to first-order transitions. *Physical Review. E, Statistical, Nonlinear, and Soft Matter Physics, 84*(6). https://doi.org/10.1103/PhysRevE.84.066116
Huang, Z., Wang, C., Nayak, A., & Stojmenovic, I. (2015). Small Cluster in Cyber Physical Systems: Network Topology, Interdependence and Cascading Failures. *IEEE Transactions on Parallel and Distributed Systems, 26*(8), 2340–2351.
Iooss, B., & Saltelli, A. (2015). Introduction: Sensitivity analysis. *Handbook of Uncertainty Quantification*.
Issariyakul, T., & Hossain, E. (2012). Introduction to network simulator NS2.
Johansson, M. I., Östling, M., & Jagschies, G. (2018). Downstream Processing Equipment. *Biopharmaceutical Processing: Development, Design, and Implementation of Manufacturing Processes*.
Jung, M., Cho, J. H., & Ryu, W. (2003). LNG terminal design feedback from operator's practical improvements. *22nd World Gas Congress*.
Kim, T. (2010). Integration of Wireless SCADA through the Internet. *International Journal of Computers and Communications*.
Koch, F. H., Yemshanov, D., McKenney, D. W., & Smith, W. D. (2009). Evaluating critical uncertainty thresholds in a spatial model of forest pest invasion risk. *Risk Analysis, 29*(9), 1227–1241. https://doi.org/10.1111/j.1539-6924.2009.01251.x
Kopustinskas, V., & Praks, P. (2014). Time dependent gas transmission network probabilistic simulator: Focus on storage discharge modeling. *Safety and Reliability: Methodology and Applications*.
Korkali, M., Veneman, J. G., Tivnan, B. F., Bagrow, J. P., & Hines, P. D. H. (2017). Reducing cascading failure risk by increasing infrastructure network interdependence. *Scientific Reports, 7*(1). https://doi.org/10.1038/srep44499
Kremers, E., Gonzalez De Durana, J., & Barambones, O. (2013). Multi-agent modeling for the simulation of a simple smart microgrid. *Energy Conversion and Management, 75*, 643–650.
Linkov, I., & Kott, A. (2018). Fundamental concepts of cyber resilience: Introduction and overview. *Cyber Resilience of Systems and Networks*. Springer.
Lloyd, E. K., Bondy, J. A., & Murty, U. S. R. (2007). Graph theory with applications. *The Mathematical Gazette*.
Lv, W. D., Tian, D., Wei, Y., & Xi, R. X. (2019). Innovation resilience: A new approach for managing uncertainties concerned with sustainable innovation. *Sustain, 11*(9), 2635.
Makowski, D. (2013). Uncertainty and sensitivity analysis in quantitative pest risk assessments; practical rules for risk assessors. *NeoBiota, 18*, 157–171.
McAllister, E. W. (2005). Pipeline Rules of Thumb Handbook.
Michael, A. G., Danziger, M., Shekhtman, L. M., Bashan, A., Berezin, Y., & Havlin, S. (2016). Interconnected networks. DOI: 10.1007/978-3-319-23947-7_5.
Mohamed, N., Jawhar, I., & Shuaib, K. (2008). Reliability challenges and enhancement approaches for pipeline sensor and actor networks. *Networks (ICWN 2008)*.
Morio, J. (2011). Global and local sensitivity analysis methods for a physical system. *European Journal of Physics, 32*(6), 1577–1583.
Most, T. (2012). Variance-based sensitivity analysis in the presence of correlated input variables. *Proc. 5th Int. Conf. Reliab. Eng. Comput. (REC)*.
Neacşu, S., Suditu, S., & Stoica, D. (2014). *Considerations on transport capacity of natural gas pipelines and its limits*. Analele Universitatii "Ovidius" Constanta – Ser. Chim.
NetSCADA (2010). SCADA communications using radio, microwave, and satellite.
Oakley, S. M. J. An efficient method for computing partial expected value of perfect information for correlated inputs. pp. 1–18.
Ouyang, M. (2014). Review on modeling and simulation of interdependent critical infrastructure systems. *Reliability Engineering and System Safety, 121*, 43–60.
Pelechrinis, K., Iliofotou, M., & Krishnamurthy, S. V. (2011). Denial of service attacks in wireless networks: The case of jammers. *IEEE Communications Surveys and Tutorials., 13*(2), 245–257.
Perz, S. G., Muñoz-Carpena, R., Kiker, G., & Holt, R. D. (2013). Evaluating ecological resilience with global sensitivity and uncertainty analysis. *Ecological Modelling., 263*, 174–186.
Pete Loucks, E. V. B. (2017). An introduction to probability, statistics and uncertainty. *Water Resource Systems Planning and Management*, 213–300.
Peterson, G. L., Whitaker, T. B., Stefanski, R. J., Podleckis, E. V., Phillips, J. G., Wu, J. S., et al. (2009). A Risk Assessment Model for Importation of United States Milling Wheat Containing Tilletia contraversa. *Plant Disease, 93*(6), 560–573. https://doi.org/10.1094/PDIS-93-6-0560
Peterson, G. L., Whitaker, T. B., Stefanski, R. J., Podleckis, E. V., Phillips, J. G., Wu, J. S., et al. (2009). A Risk Assessment Model for Importation of United States Milling Wheat Containing Tilletia contraversa. *Plant Disease, 93*(6), 560–573. https://doi.org/10.1094/PDIS-93-6-0560
Pianosi, F., Sarrazin, F., & Wagener, T. (2015). A Matlab toolbox for Global Sensitivity Analysis. *Environ. Model. Softw., 70*, 80–85.
Pipeline Pressure Limits. http://www.hse.gov.uk/pipelines/resources/pipelinepressure.htm.
Platt, S., Brown, D., & Hughes, M. (2016). Measuring resilience and recovery. *International Journal of Disaster Risk Reduction, 19*, 447–460. https://doi.org/10.1016/j.ijdrr.2016.05.006
Praks, P., Kopustinskas, V., & Masera, M. (2015). Probabilistic modelling of security of supply in gas networks and evaluation of new infrastructure. *Reliability Engineering & System Safety, 144*, 254–264.
Queiroz, C., Mahmood, A., & Tari, Z. (2011). SCADASim A framework for building SCADA simulations. *IEEE Trans. Smart Grid*.
Saltelli, A. et al. (2008). Global sensitivity analysis the primer. pp. 155–167.
Saltelli, A., & Tarantola, S. (2002). On the Relative Importance of Input Factors in Mathematical Models. *Journal of American Statistical Association, 97*(459), 702–709. https://doi.org/10.1198/016214502388618447
Saltelli, A., Tarantola, S., Campolongo, F., & Ratto, M. (2004). *Sensitivity Analysis in Practice: A Guide to Assessing Scientific Models*. Wiley.
Sayfayn, S.M.N. Cybersafety Analysis of the Maroochy Shire Sewage Spill.
Schreider, S., Plummer, J., & Miller, B. M. (2015). Sensitivity analysis of gas supply optimization models. DOI: 10.1007/s10479-014-1709-0.
Sobol, I. M. (1993). Sensitivity estimates for nonlinear mathematical models. Mathematical modeling and computational experiment.
Su, H., Zhang, J., Zio, E., Yang, N., Li, X., & Zhang, Z. (2018). An integrated systemic method for supply reliability assessment of natural gas pipeline networks. *Applied Energy, 209*, 489–501.
Su, H., Zio, E., Zhang, J., Yang, Z., Li, X., & Zhang, Z. (2018). A systematic hybrid method for real-time prediction of system conditions in natural gas pipeline networks. *Journal of Natural Gas Science and Engineering, 57*, 31–44.
Tierney, K., & Bruneau, M. (2007). A key to disaster loss reduction. *TR News*.
Transmission Europe. Definition of available capacities at interconnection points in liberalized market. Ref.: 04CA041-final.
Wadhawan, Y., & Neuman, C. (2016). Evaluating resilience of gas pipeline systems under cyber-physical attacks. DOI: 10.1145/2994487.2994488.
Wadhawan, A. A. M. Y., & Neumann, C. (2018). A systematic approach for analyzing multiple cyber-physical attacks on the smart grid. *Int. J. Comput. Inf. Eng., 12*.
Wilkinson, G., & David, R. (2009). Back to basics: Risk matrices and ALARP. *Safety-Critical Systems: Problems, Process and Practice – Proceedings of the 17th Safety-Critical Systems Symposium, SSS*.
Zeng, J., Sun, C., Zhu, Z., Wu, J., & Chen, H. (2018). Uncertainty Analysis for Natural Gas Transport Pipeline Network Layout: A New Methodology Based on Monte Carlo Method. *Journal of Advanced Transportation*. https://doi.org/10.1155/2018/9213648. Article ID 9213648, 10 pages.
Zhang, X., Mahadevan, S., Sankararaman, S., & Goebel, K. (2018). Resilience-based network design under uncertainty. *Reliability Engineering & System Safety, 169*, 364–379.
Zio, E. (2007). *An introduction to the basics of reliability and risk analysis* (Vol. 13). World Scientific.
Zio, E. (2009). *Computational methods for reliability and risk analysis* (Vol. 14). World Scientific.
Zio, E., & Pedroni, N. (2010). Sensitivity analysis of the model of a nuclear passive system by means of subset simulation. *Procedia - Social and Behavioral Sciences, 2*(6), 7778–7779.
Zio, E., & Pedroni, N. (2012). Monte Carlo simulation-based sensitivity analysis of the model of a thermal-hydraulic passive system. *Reliability Engineering and System Safety, 107*, 90–106.
Zio, E., & Sansavini, G. (2013). Vulnerability of Smart Grids with Variable Generation and Consumption: A System of Systems Perspective. *IEEE Transactions on Systems, Man and Cybernetics, Part A: Systems and Humans Institute of Electrical and Electronics Engineers, 43*(3), 477–487.